

Looking for evidence of color decoherence in jet observables

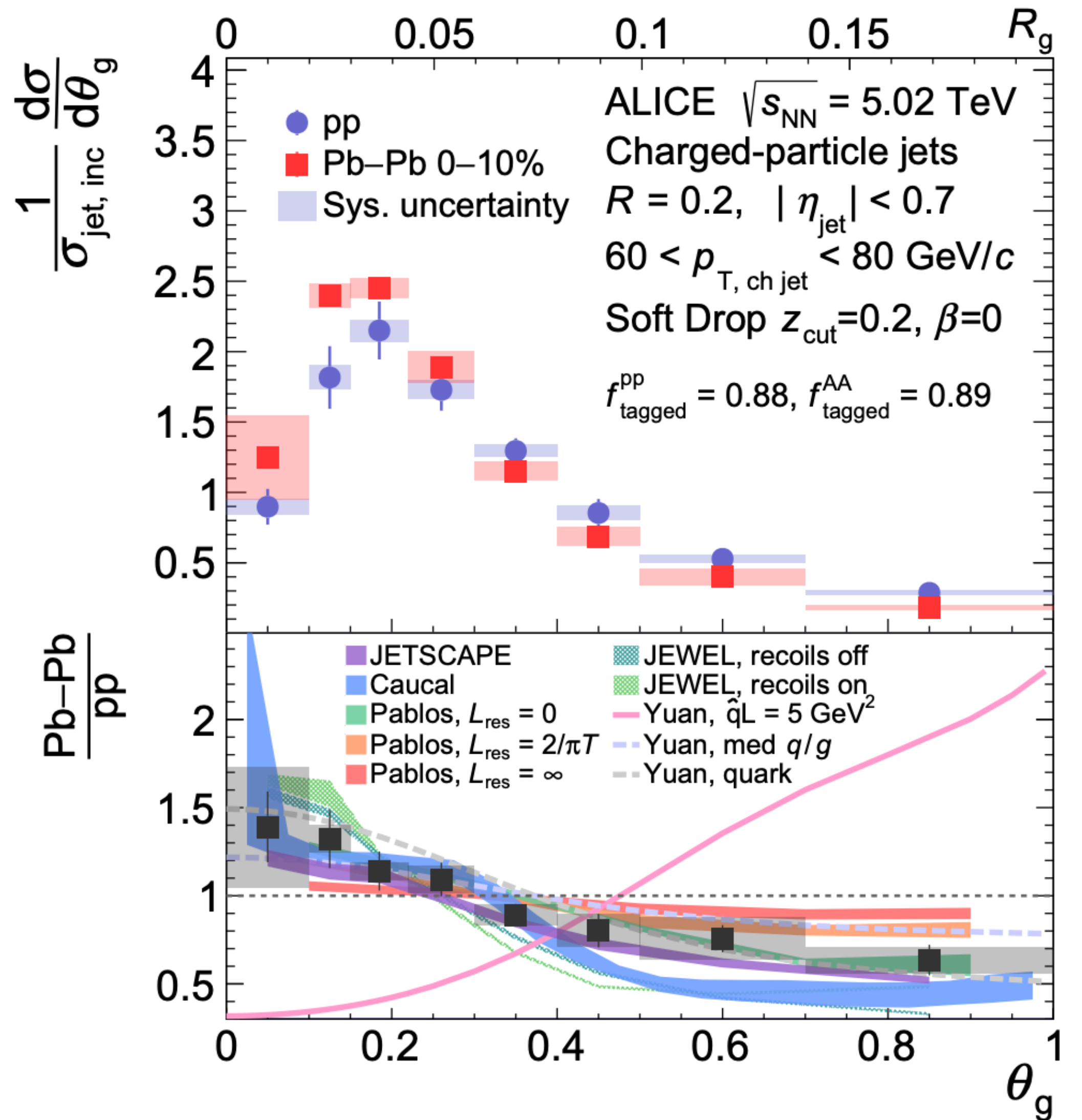
Daniel Pablos



This project has received funding from the European Union's Horizon 2020 research and innovation programme under the Marie Skłodowska-Curie grant agreement n. 754496.

QCD challenges from pp to AA collisions
13th Feb. 2023

Narrowing of Jet Substructure



ALICE - PRL '22

Example: Groomed radius.

Many Monte Carlo models get similar results.

Bias towards narrower, less active jets.

Medium q/g can also account for the signal.

Strong suppression of gluon jets (factor 4 w.r.t. pp).

Qiu et al. - PRL '19

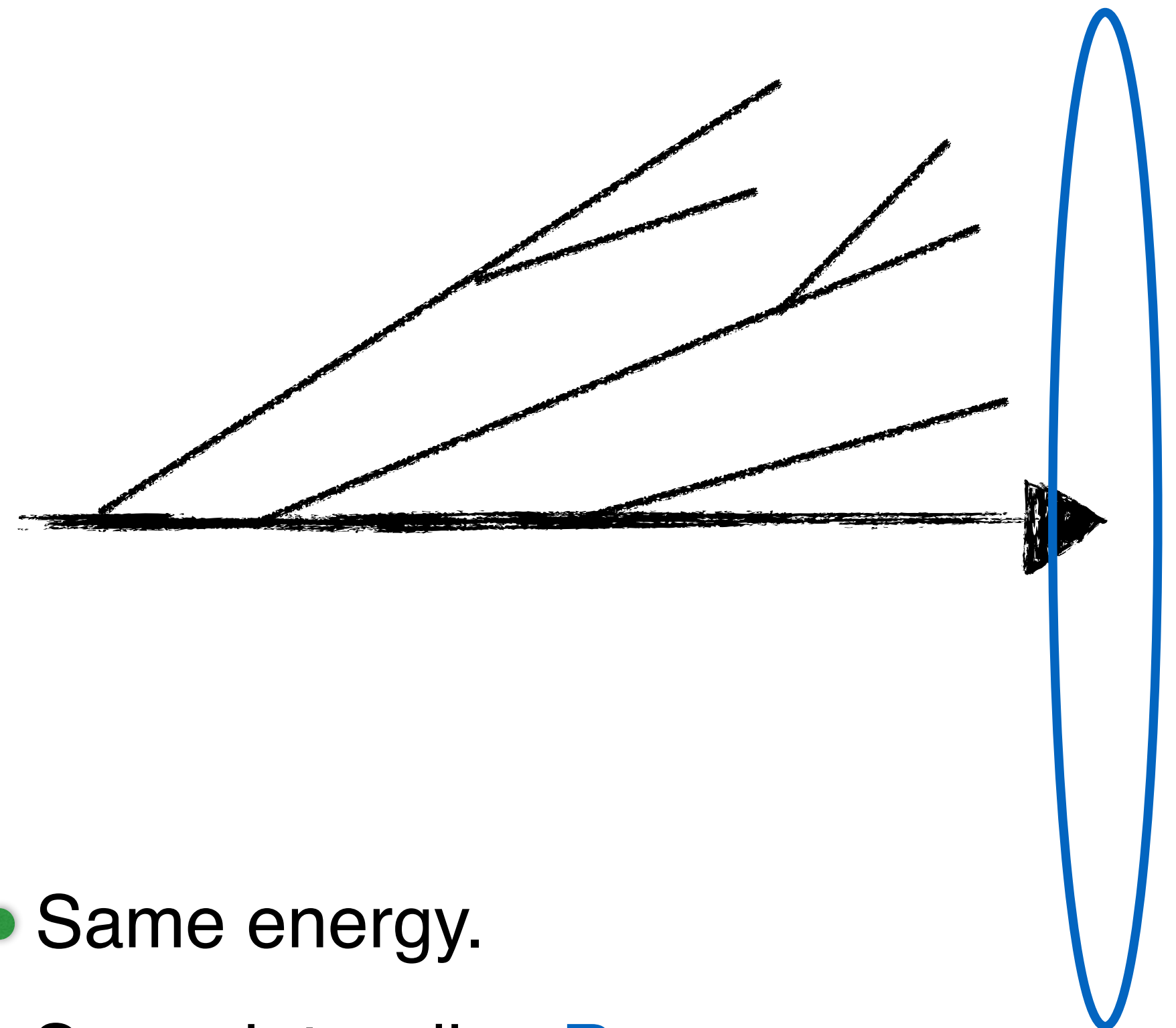
Medium q/g + p_T broadening fails.

Not accounting for selection bias, while broadening emissions, results in a broader jet ensemble.

Ringer et al. - PLB '19

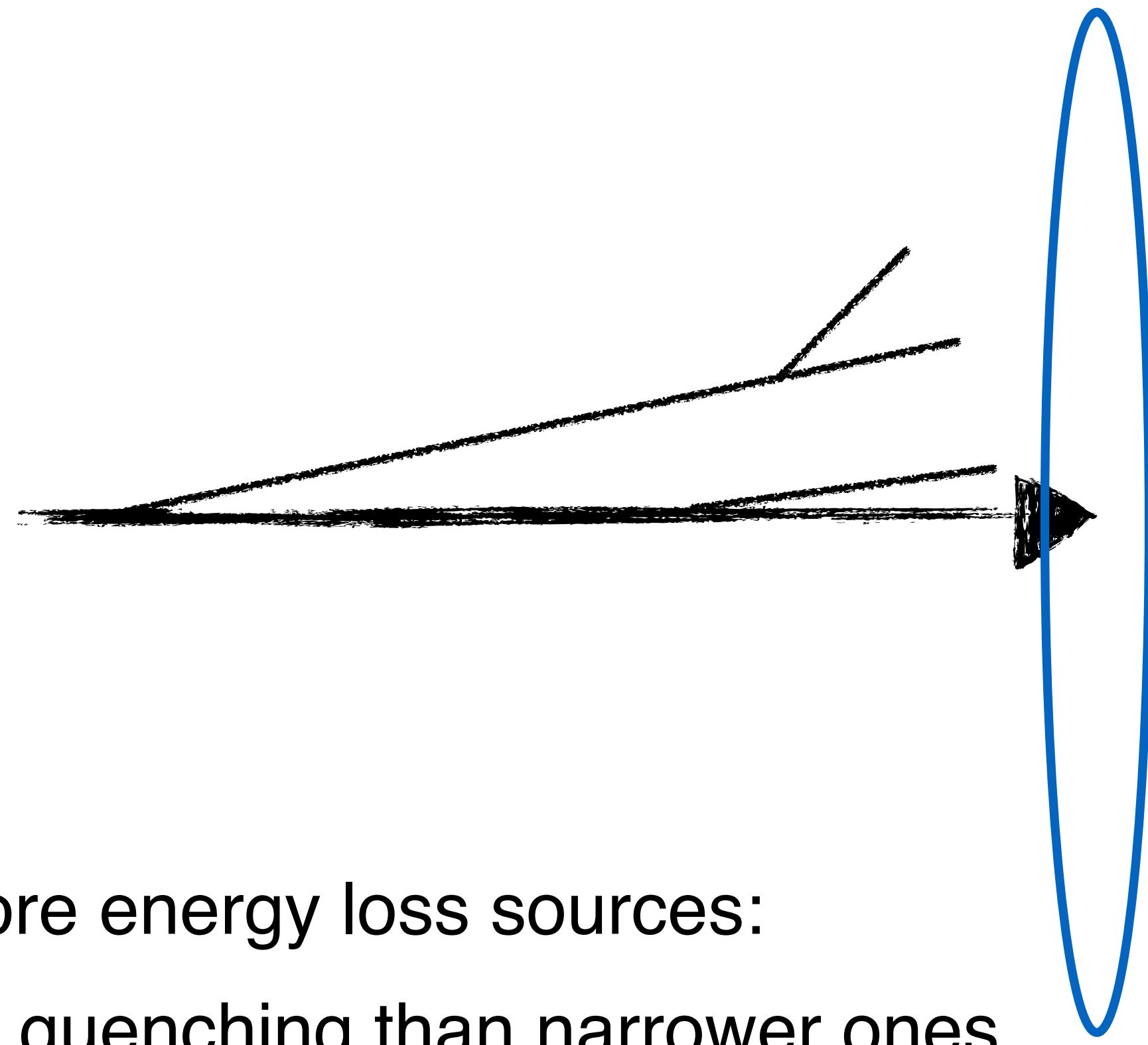
Jets and Jets

Wide jet



- Same energy.
- Same jet radius R .
- Different fragmentation pattern.

Narrow jet



Wider jets have more energy loss sources:

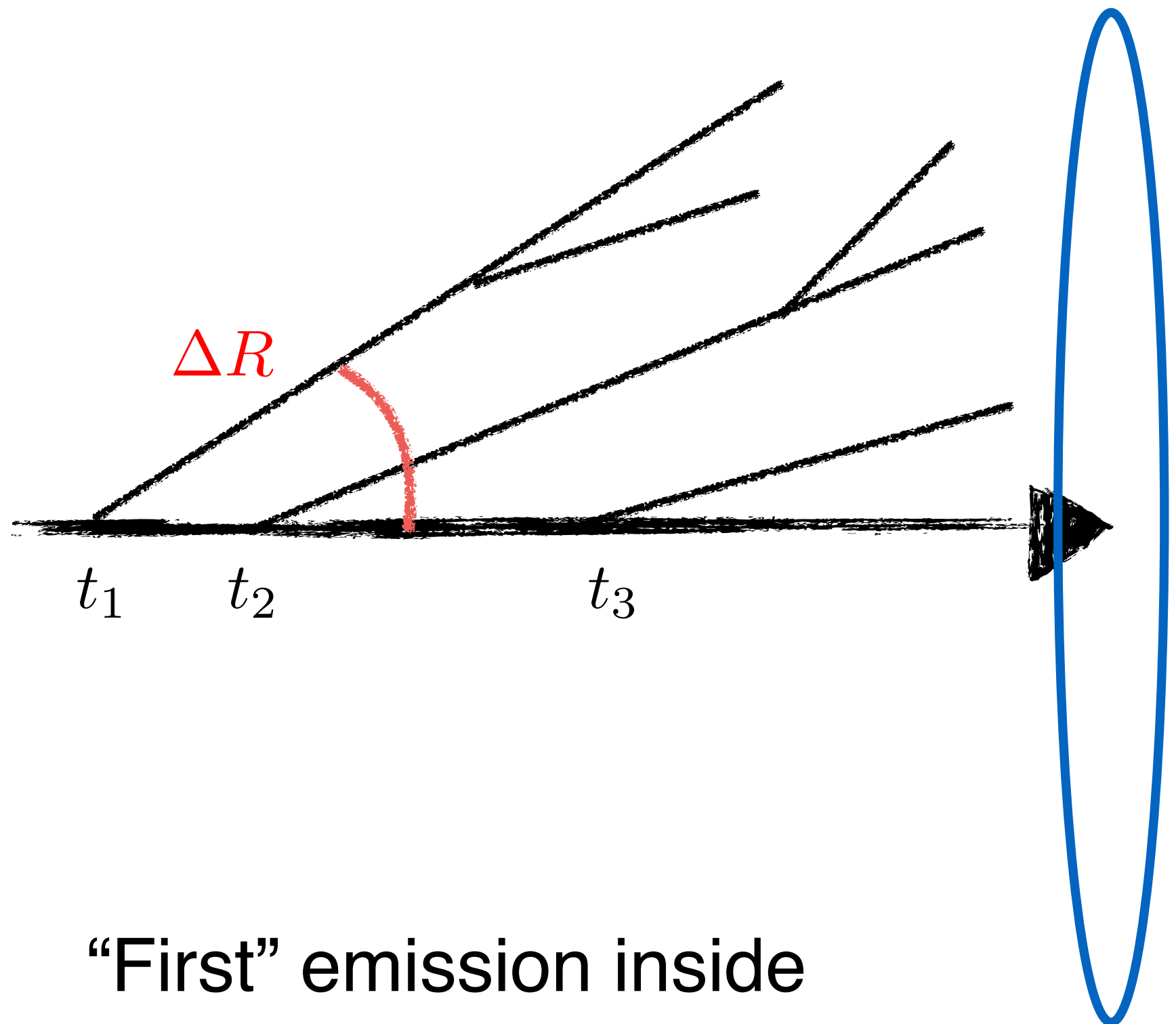
→ more total quenching than narrower ones.

Assuming:

- most of the energy goes out of the cone.
- internal structure resolved by QGP.

Jets and Jets

Wide jet



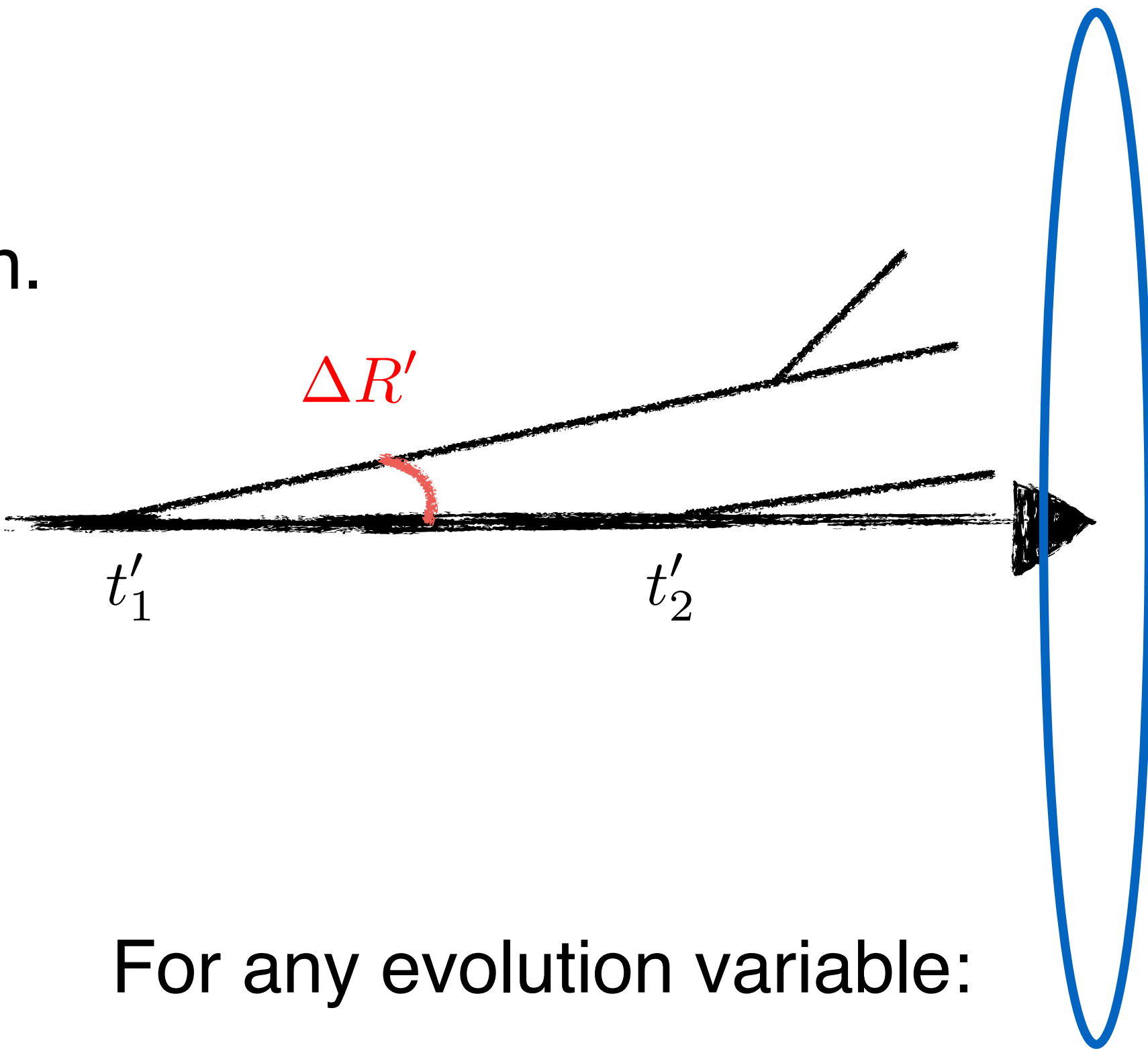
“First” emission inside
the jet cone determines
available phase space
for further in-cone emissions.

Groomed angle is
proxy for jet activity.

Scale of emission t
sampled from
Sudakov distribution.

$$t_1 > t'_1$$

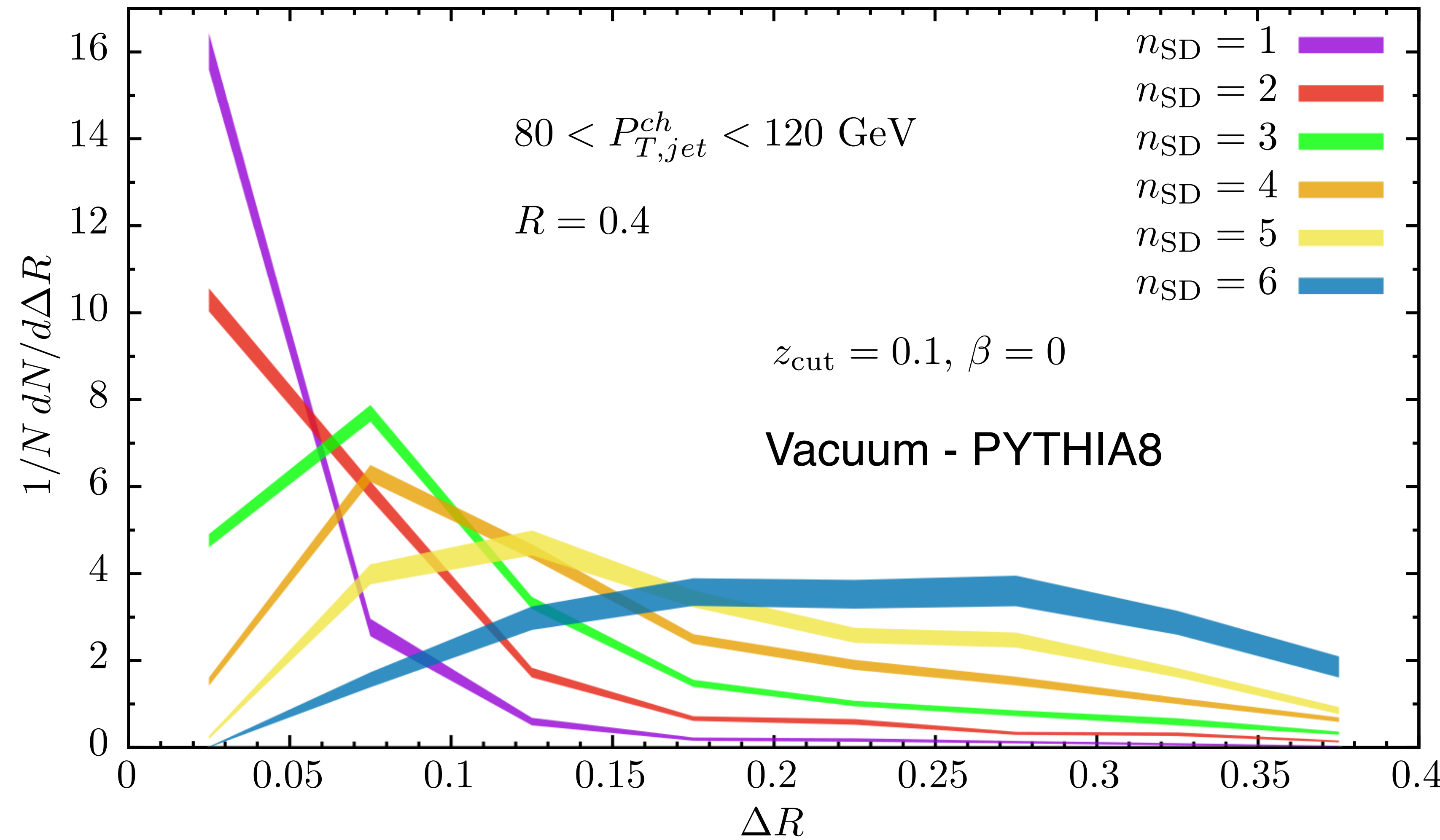
Narrow jet



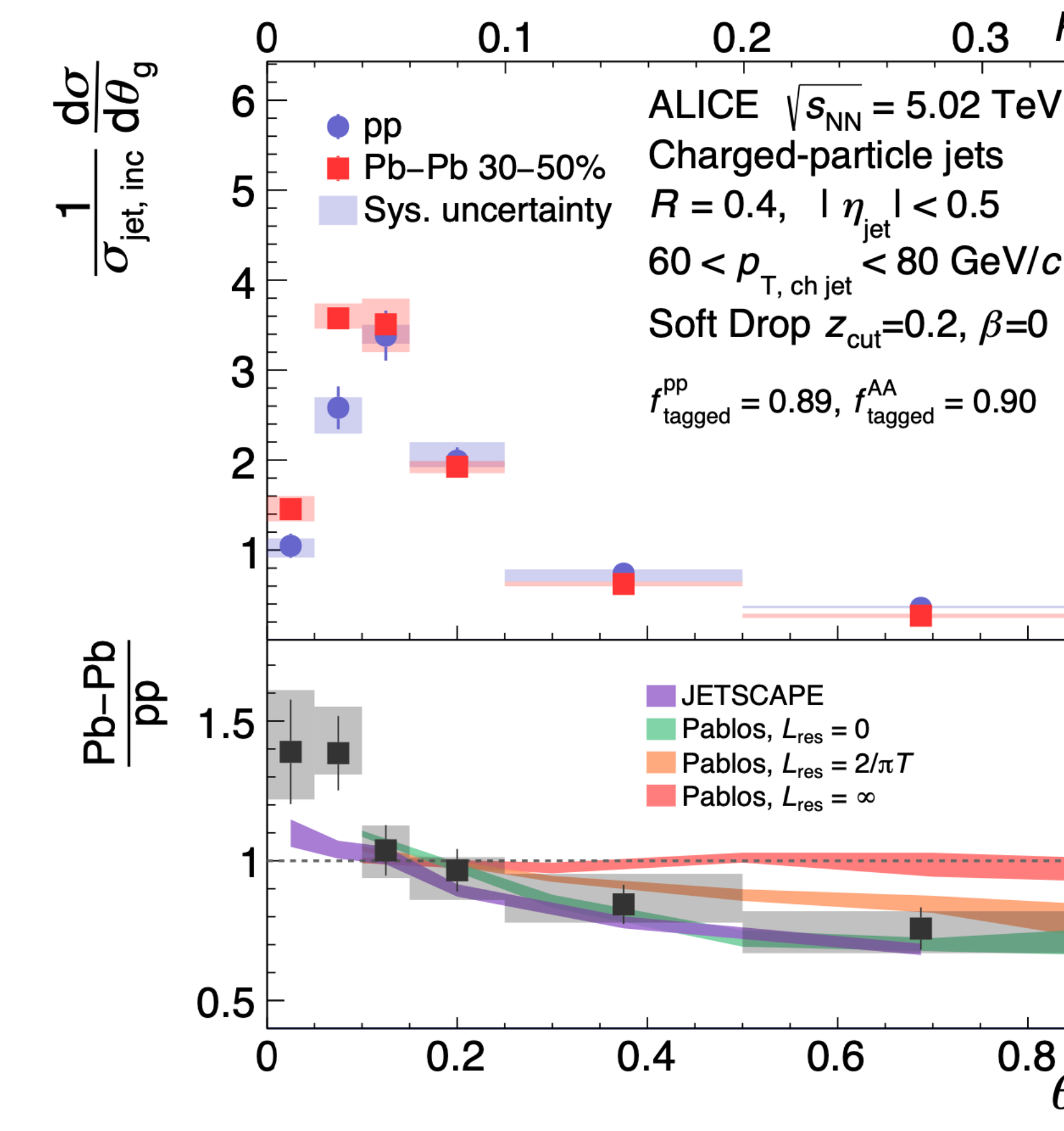
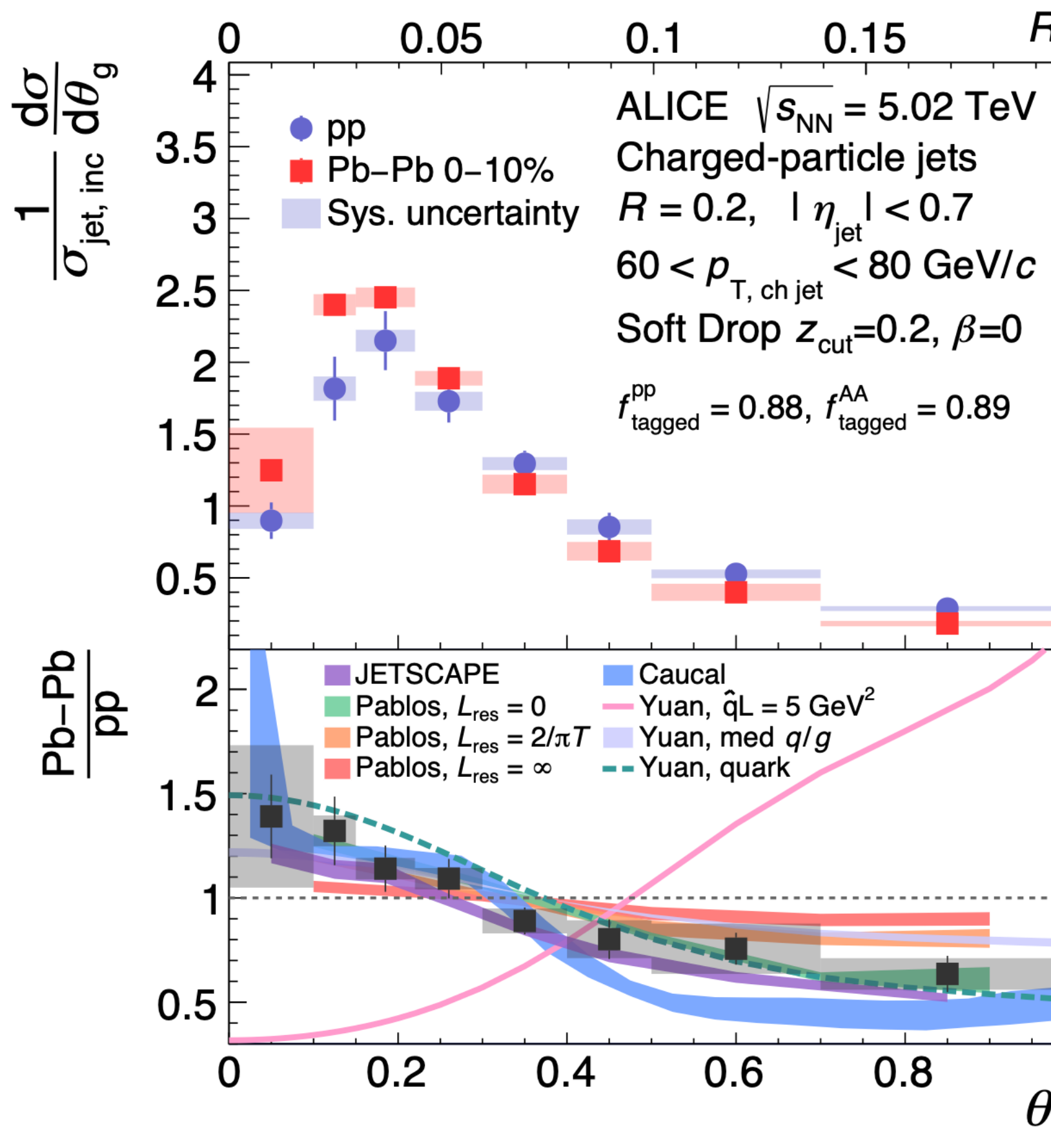
For any evolution variable:

$$\begin{aligned} t_1 &\propto \Delta R \\ t'_1 &\propto \Delta R' \end{aligned}$$

Correlation between n_{SD} and ΔR



Common feature among MC models



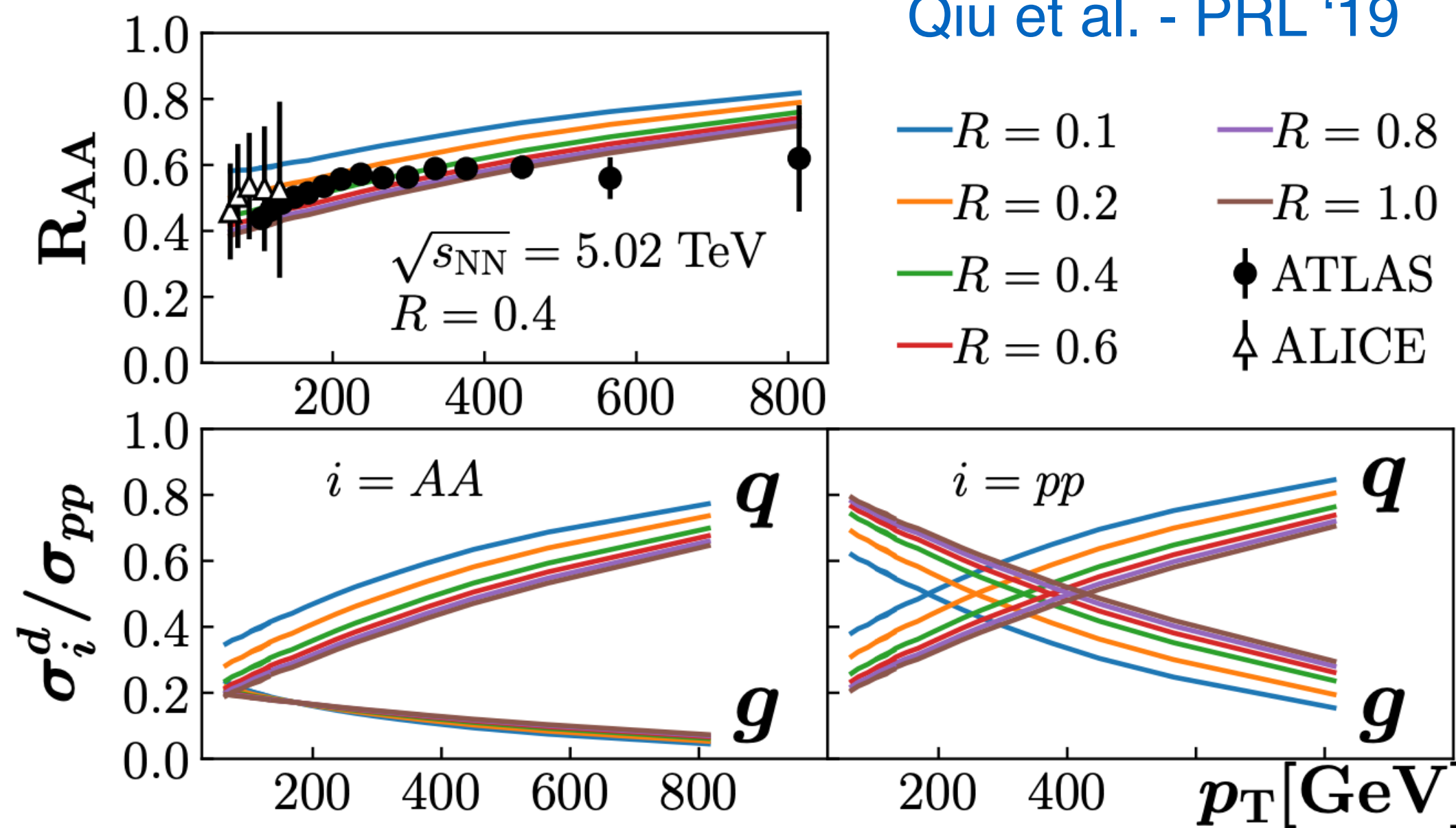
ALICE - PRL '22

ΔR narrowing observed
in data, well reproduced by
variety of models.

Most relevant common feature between MCs:

→ dominance of vacuum physics at early, high energy stages of the shower.

Modified q/g Fraction



- Combination of quark and gluon contributions:

$$\frac{1}{\sigma_{\text{incl}}} \frac{d\Sigma(\theta_g)}{dp_T d\eta} = f_q \Sigma_q(\theta_g) + f_g \Sigma_g(\theta_g)$$

- Broadening added as non-perturbative kick.

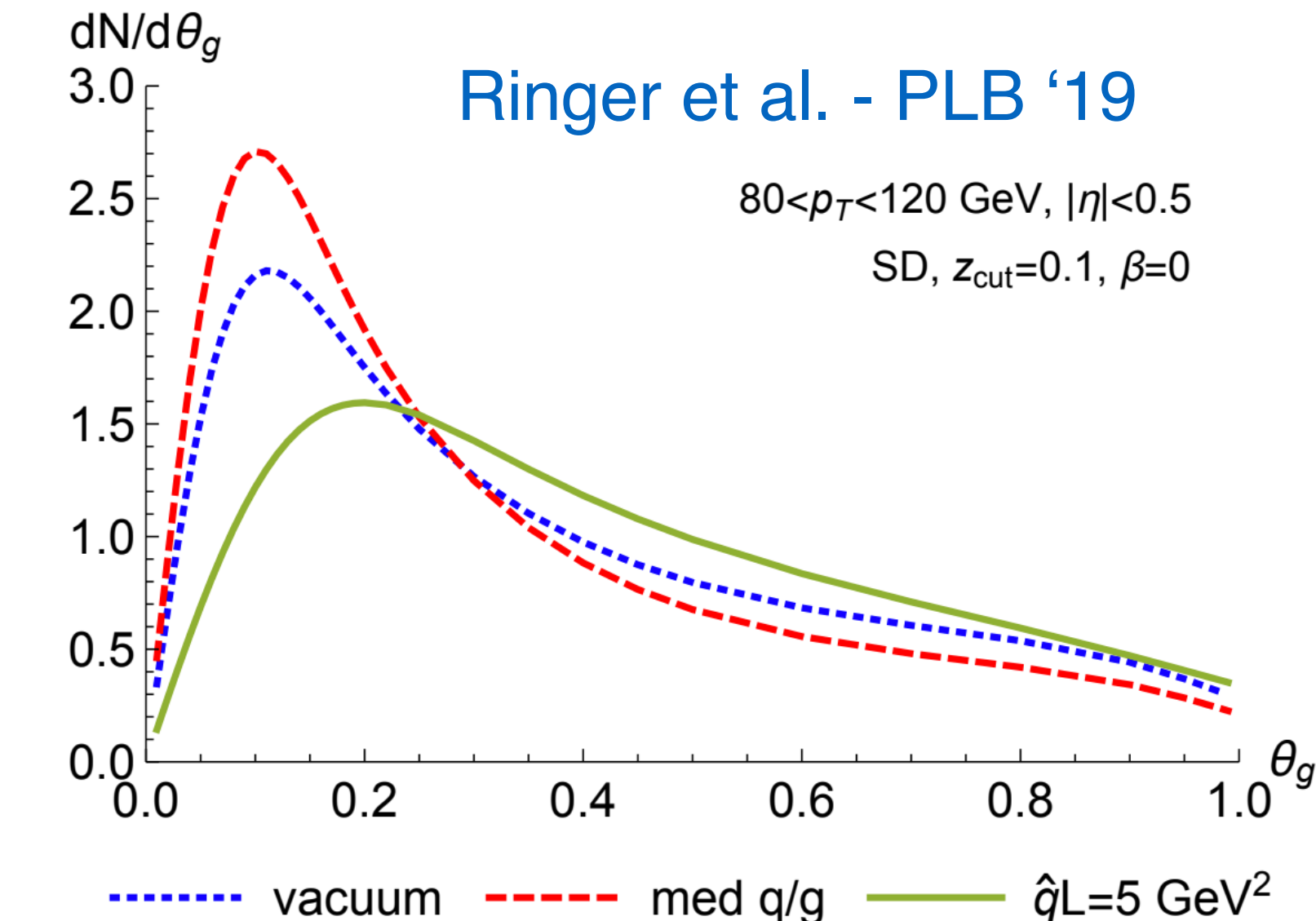
- Parametrization of modification of jet function (similar to nPDF).

$$\mu \frac{d}{d\mu} J_c(z, p_T R, \mu) = \sum_d P_{dc}(z) \otimes J_d(z, p_T R, \mu)$$

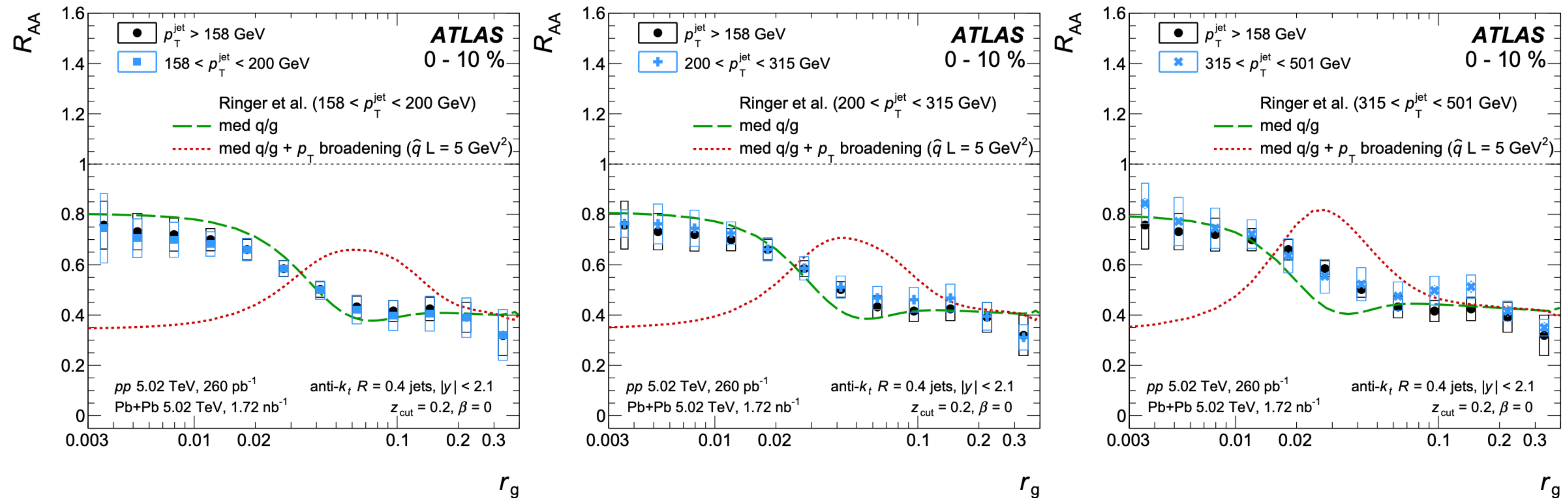
$$J_c^{\text{med}}(z, p_T R, \mu_J) = W_c(z) \otimes J_c(z, p_T R, \mu_J)$$

$$W_c(z) = \epsilon_c \delta(1-z) + N_c z^{\alpha_c} (1-z)^{\beta_c}$$

→ Best fit seems to leave quark jets untouched.



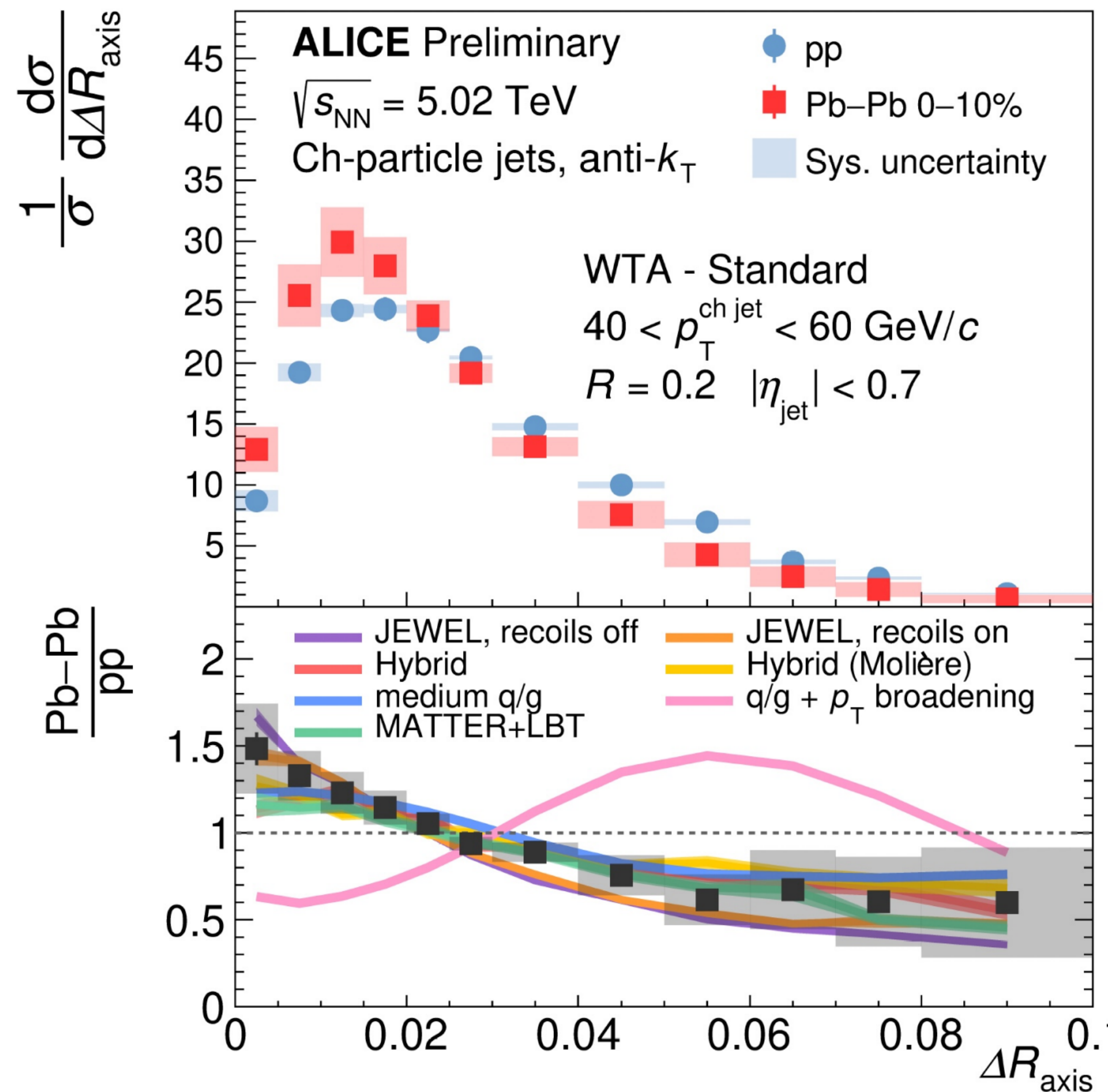
Substructure dependent jet suppression



ATLAS - 2211.11470

- Recent ATLAS results for R_{AA} vs r_g can also be explained by modified q/g fraction model.

Narrowing of Jet Substructure



R. Cruz-Torres talk at QM22

Another example: WTA axis distance w.r.t. anti- k_T axis

How can we discriminate between:

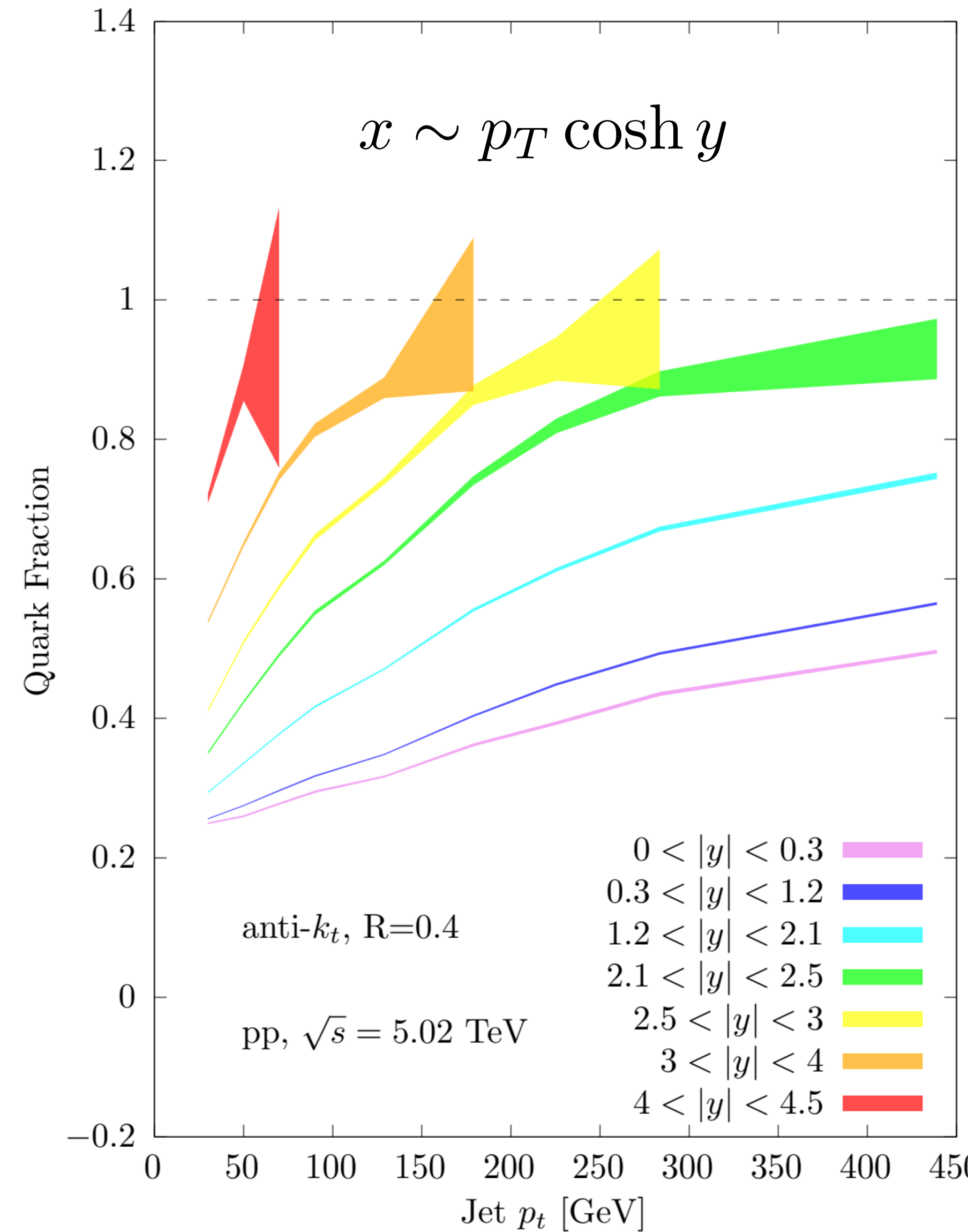
- Quenching of wider jets, either quark or gluon (medium sensitive to jet substructure fluctuations).
- Modification of q/g fraction (medium sensitive to total charge only).

Simple proposal:

→ Use an **enriched quark sample**, so that over-quenching of gluons has very little effect.

Rapidity Evolution of Quark Fraction

DP & A. Soto-Ontoso - 2210.07901



- Quark enriched samples can be obtained from e.g. inclusive b-tagged jets, semi-inclusive boson-jets.
- Here: exploit **rapidity evolution of quark fraction** to engineer quark enriched samples.

Extended rapidity coverages available in future detector upgrades.

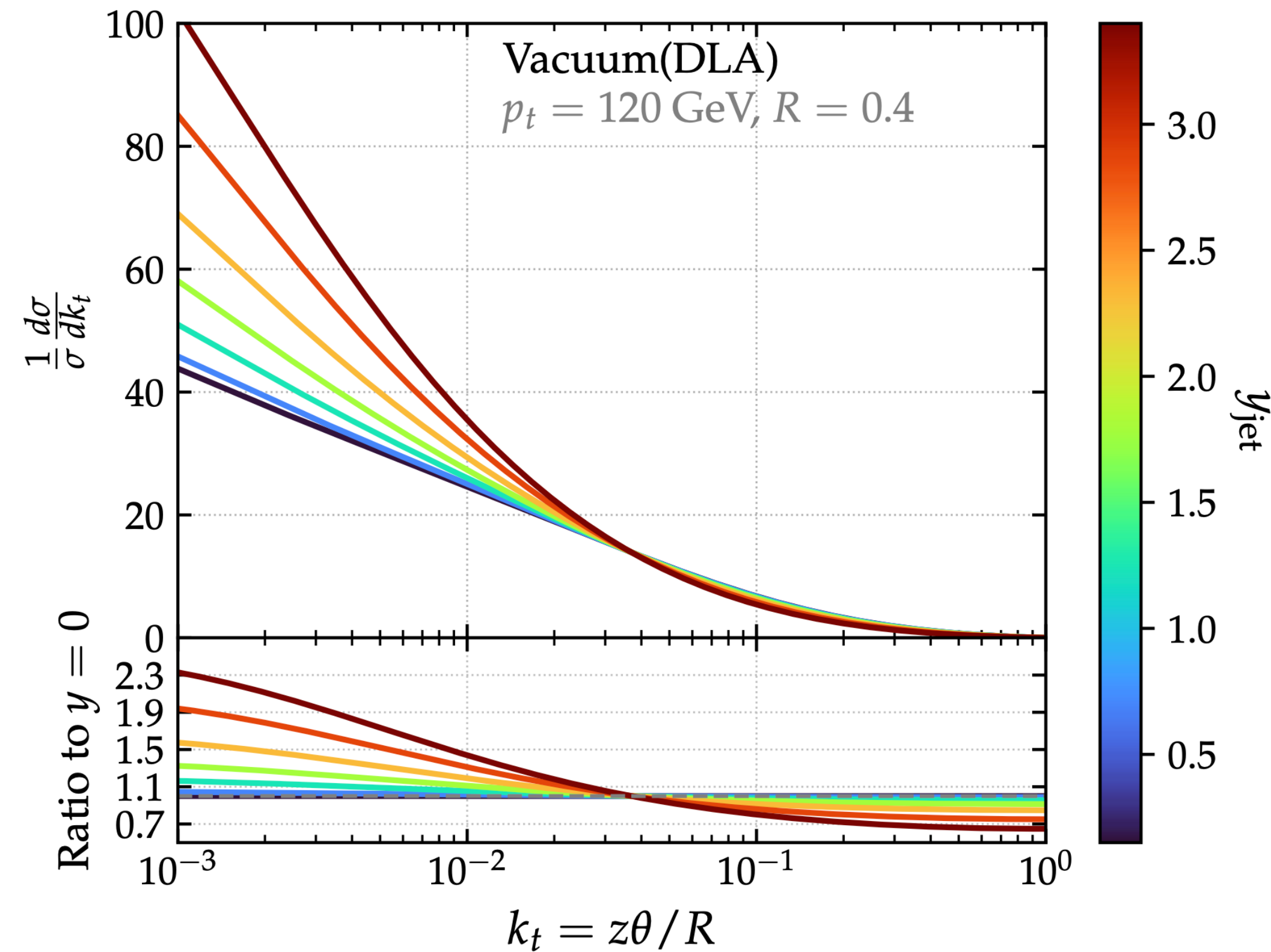


Run 5 with $|\eta| < 4$ and great p_T resolution.

CERN-LHCC-2022-009

Also ATLAS and CMS.

Leading- k_t at DLA in Vacuum



$$\frac{1}{\sigma} \frac{d\sigma}{dk_t} \Big|_{p_t, y} = \sum_{i \in \{q, g\}} f_i \int_0^1 dz \int_0^R d\theta P^{\text{vac}}(z, \theta) \delta(k_t - z\theta)$$

$$\times e^{- \int dz' \int d\theta' P^{\text{vac}}(z', \theta') \Theta(z'\theta' - k_t)}$$

$$\stackrel{\text{DLA}}{=} \sum_{i \in \{q, g\}} f_i \frac{2\bar{\alpha}}{k_t} \ln \frac{R}{k_t} e^{-\bar{\alpha} \ln^2 \frac{R}{k_t}}$$

$$\bar{\alpha} \equiv \alpha_s(p_t R) C_i / \pi$$

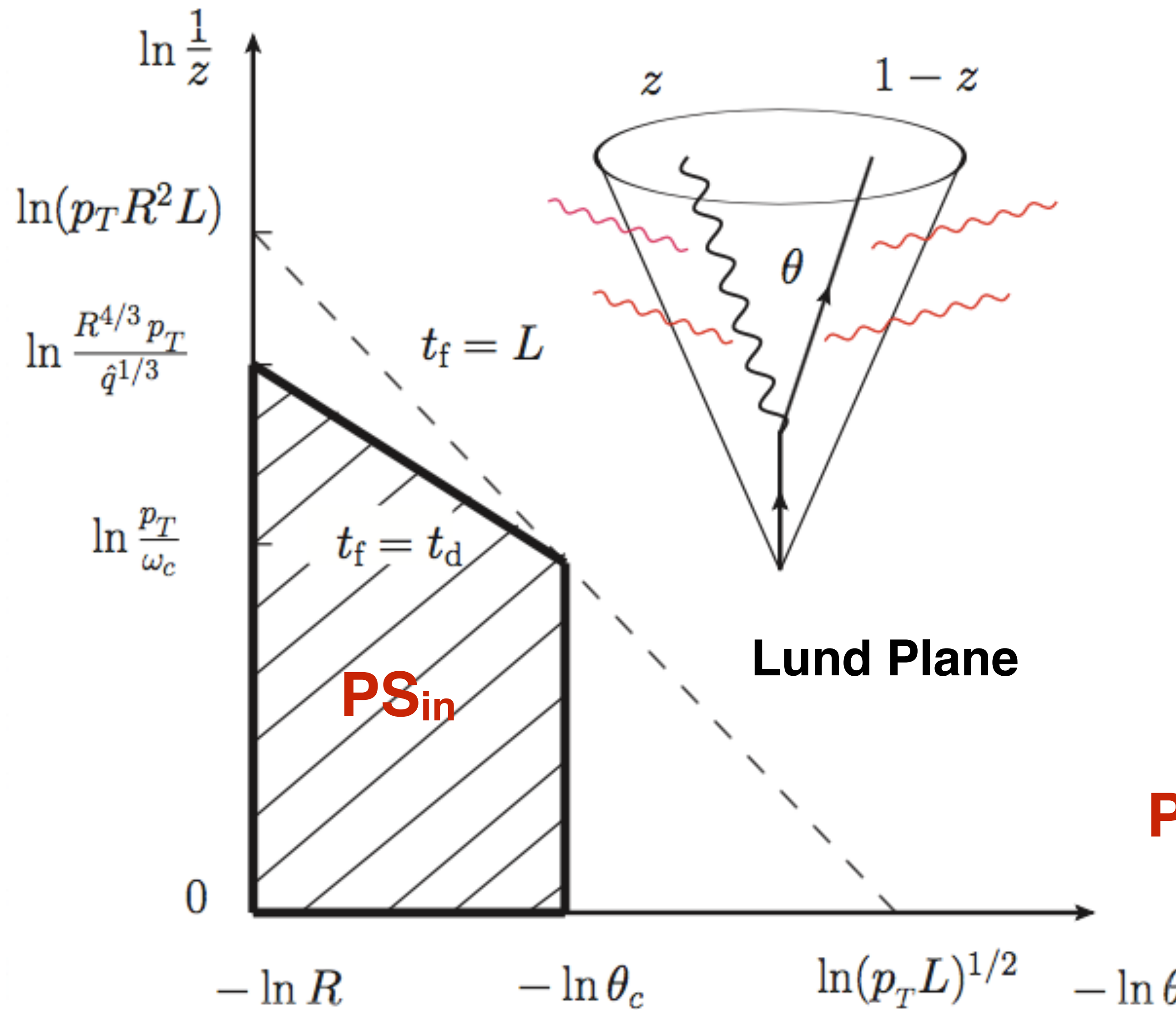
Vacuum q/g fractions; taken from PYTHIA8.

Probability of measuring splitting with k_t .

Probability there is no other splitting with larger value of k_t (Sudakov factor).

Total distribution becomes narrower at forward rapidities as q-fraction increases.

Quenched Phase Space of a Jet



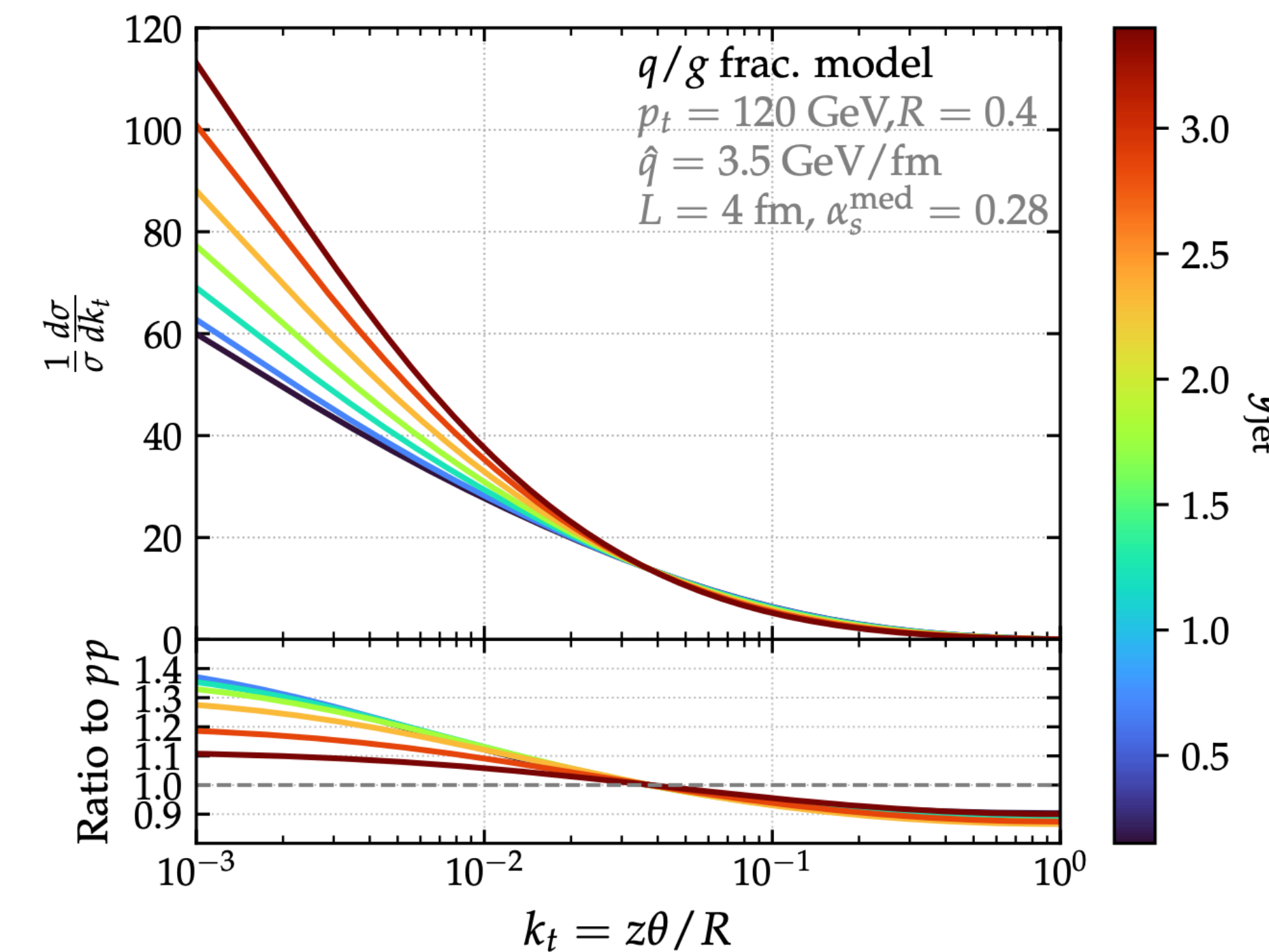
- Only those jet modes that:
 - are formed inside the medium, and, $t_f < L$
 - are resolved by the medium, $t_f < t_d$
- contribute to double-logarithmic enhancement of quenched phase space:

$$\mathbf{PS}_{\text{in}} = \bar{\alpha} \int_{t_f < t_d < L} \frac{d\theta}{\theta} \int \frac{dz}{z} \equiv \bar{\alpha} \ln \frac{R}{\theta_c} \left(\ln \frac{p_T}{\omega_c} + \frac{2}{3} \ln \frac{R}{\theta_c} \right)$$

Mehtar-Tani, Tywoniuk - PRD '18
see also Caucal, Iancu, Mueller, Soyez - PRL '18

Analytic Estimates at DLA - Summary

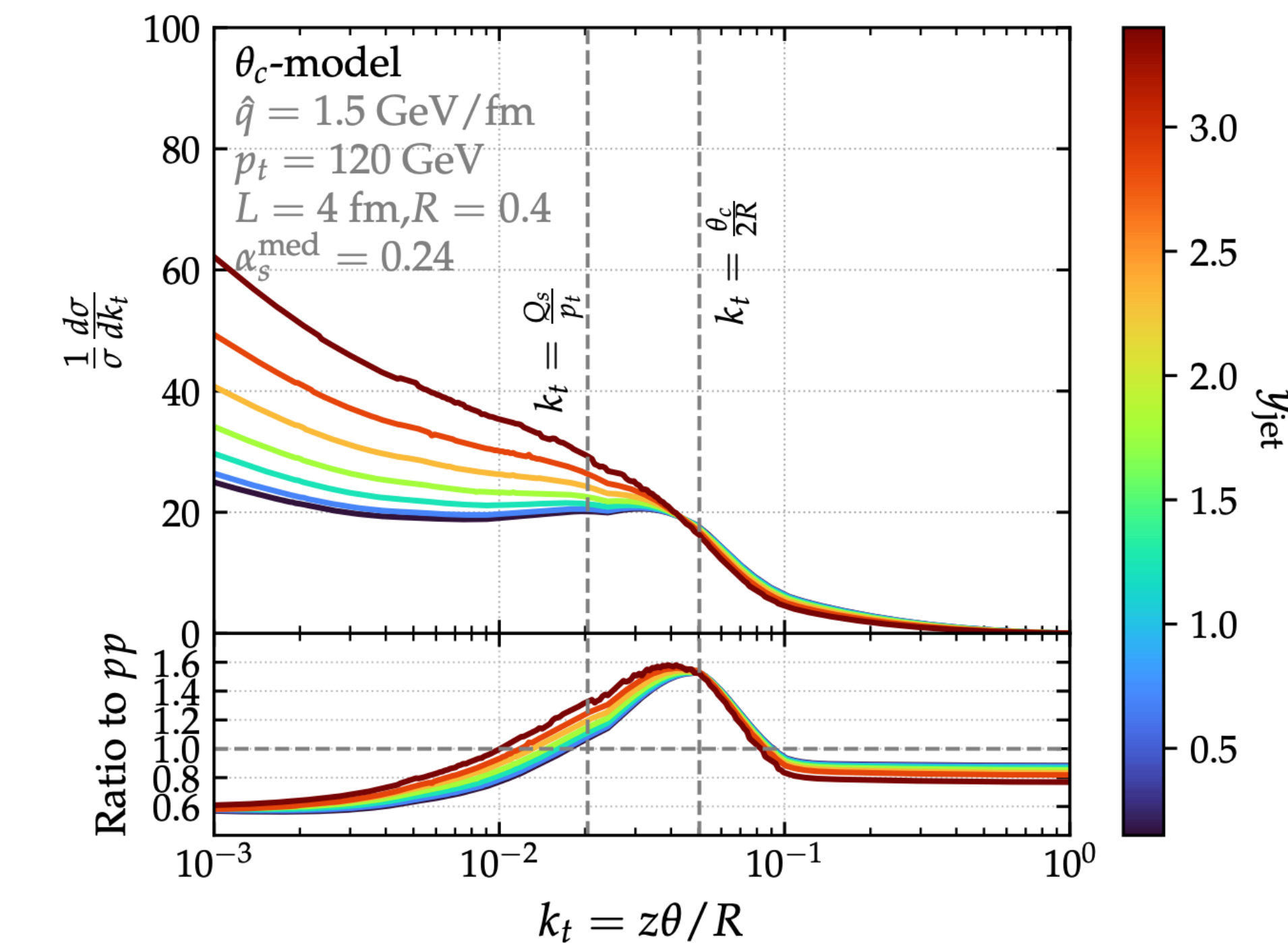
DP & A. Soto-Ontoso - 2210.07901



q/g frac model:

→ Quenching of leading charge only.

Less narrowing with increasing rapidity.



θ_c model:

→ Quenching of leading and tagged prongs if resolved (i.e. with $\theta > \theta_c$).

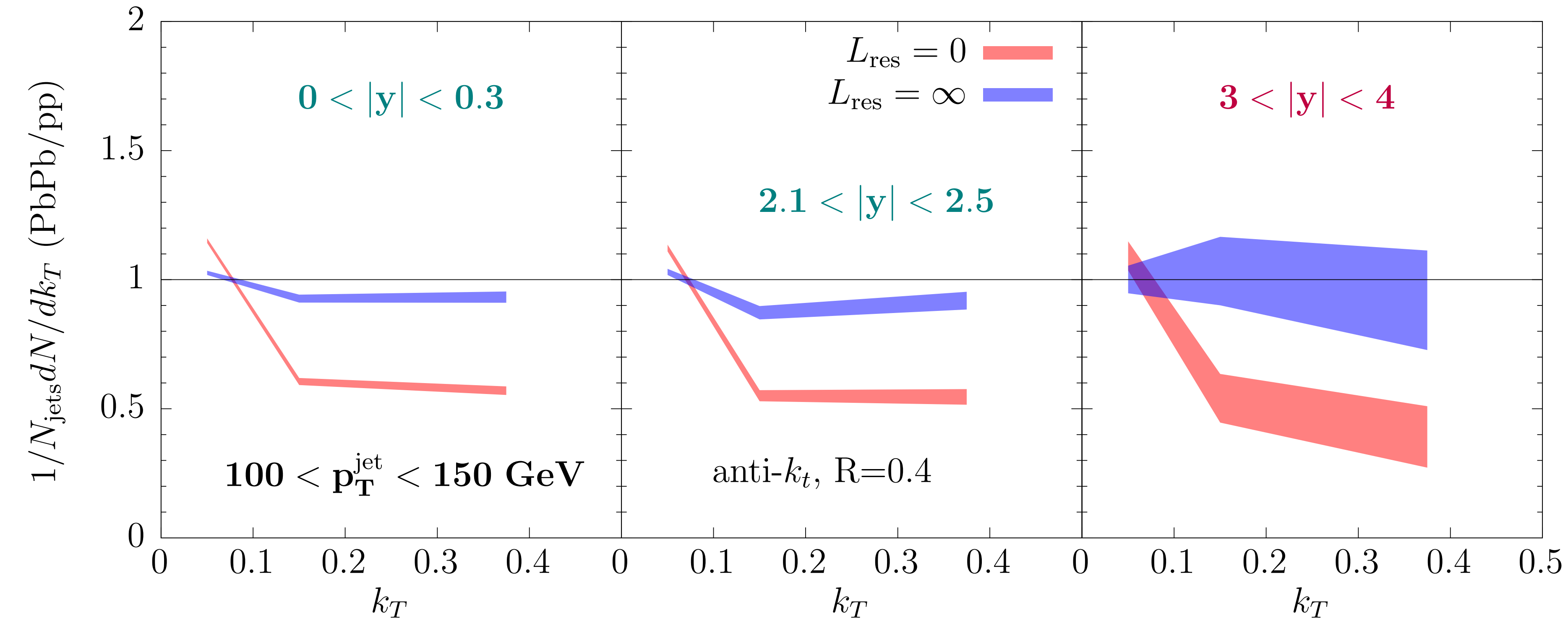
Narrowing persists also at forward rapidities.

Hybrid Model - Jet Quenching MC

0-5% Centrality

Using statistics projected for HL-LHC

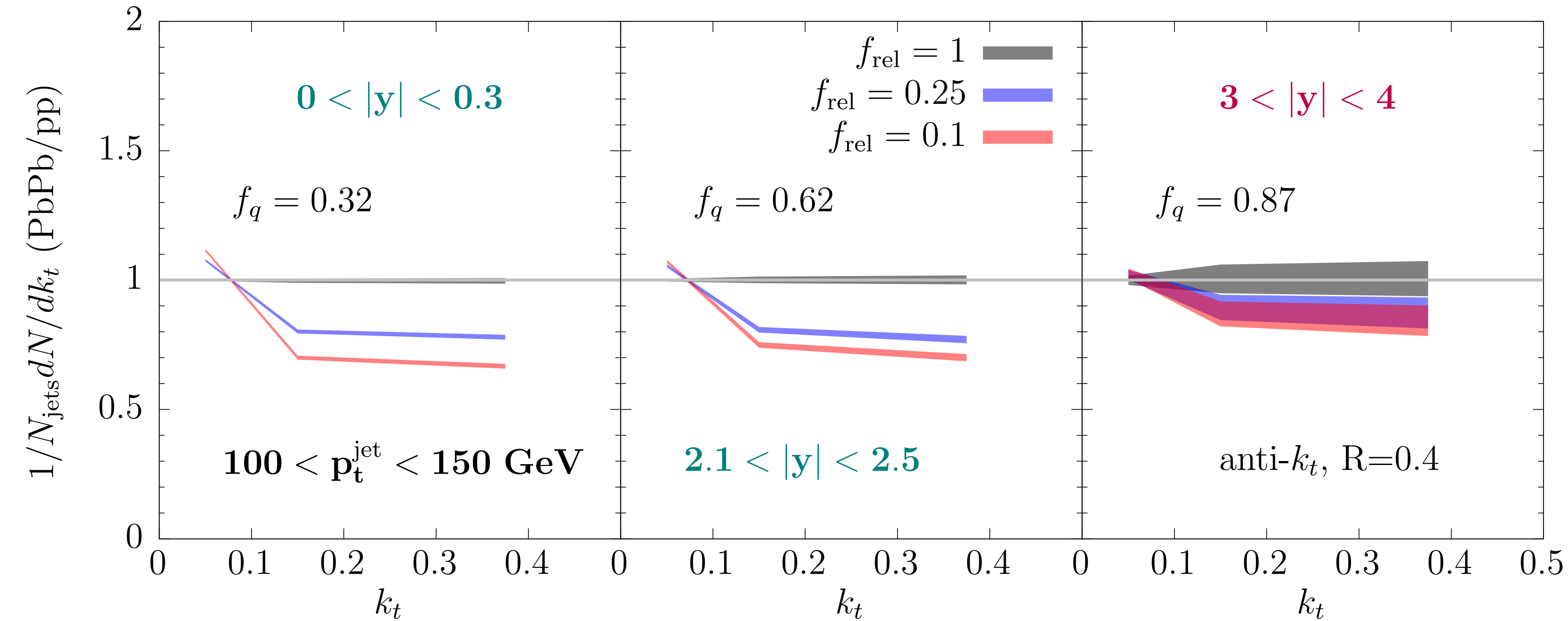
$$k_t \equiv z(p_t^{\text{parent}}/p_t^{\text{jet}}) \sin \theta / R$$



- Small effect from total charge quenching ($L_{\text{res}} = \infty$) at mid-rapidity.
- Narrowing persists at forward rapidities if jet substructure resolved ($L_{\text{res}}=0$).

Toy q/g Fraction Model

Using statistics projected for HL-LHC



BDMPS-Z:
 $f_{\text{rel}} = Q_q^{C_A/C_F - 1}$
 $f_{\text{rel}} \approx 0.5$.
 for $Q_q = 0.6$

$$\frac{1}{\sigma} \frac{d\sigma}{dk_t} \Big|_{AA} = \mathcal{N}^{-1} \left[f_q \frac{d\sigma_q}{dk_t} \Big|_{pp} + f_{\text{rel}}(1 - f_q) \frac{d\sigma_g}{dk_t} \Big|_{pp} \right]$$

Combine quark and gluon pp templates
with modified q/g fraction.

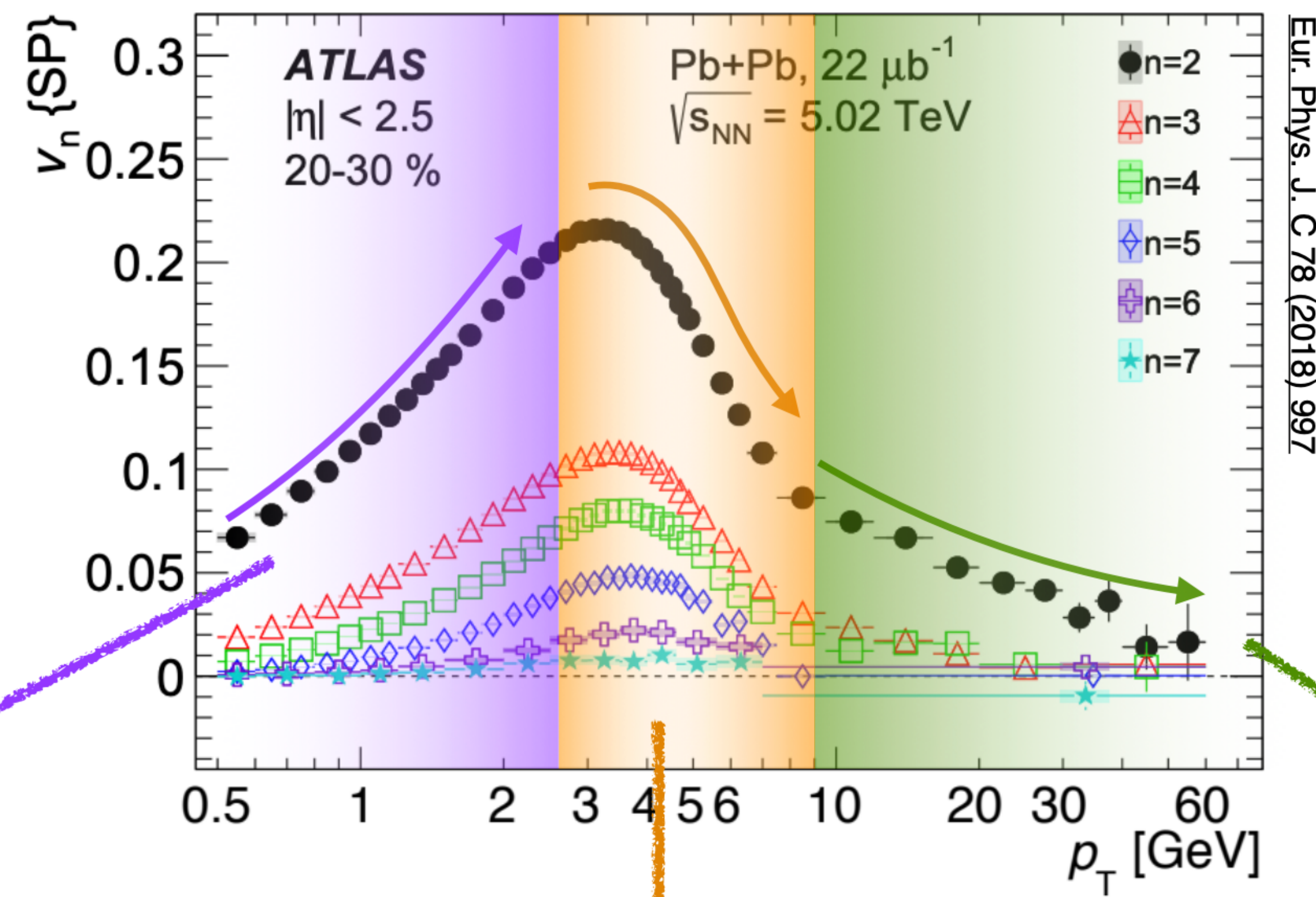
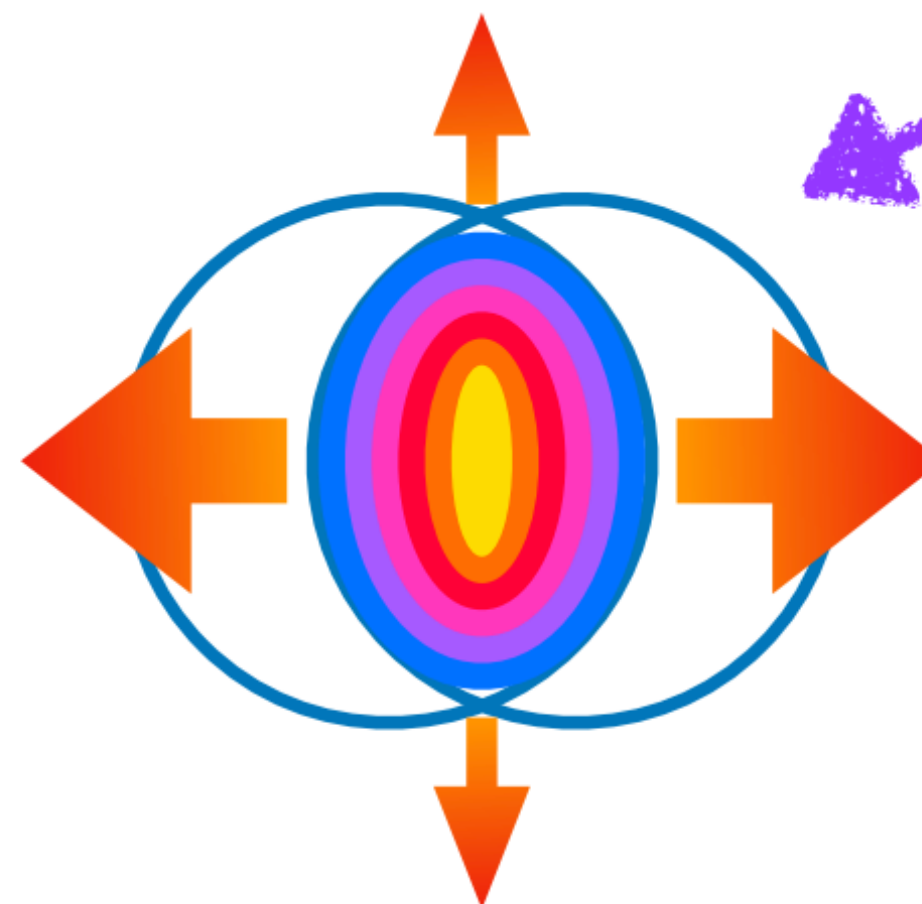
- Strong narrowing observed at mid-rapidity fades away toward forward rapidities.

DP & A. Soto-Ontoso - 2210.07901

Jet Azimuthal Anisotropy

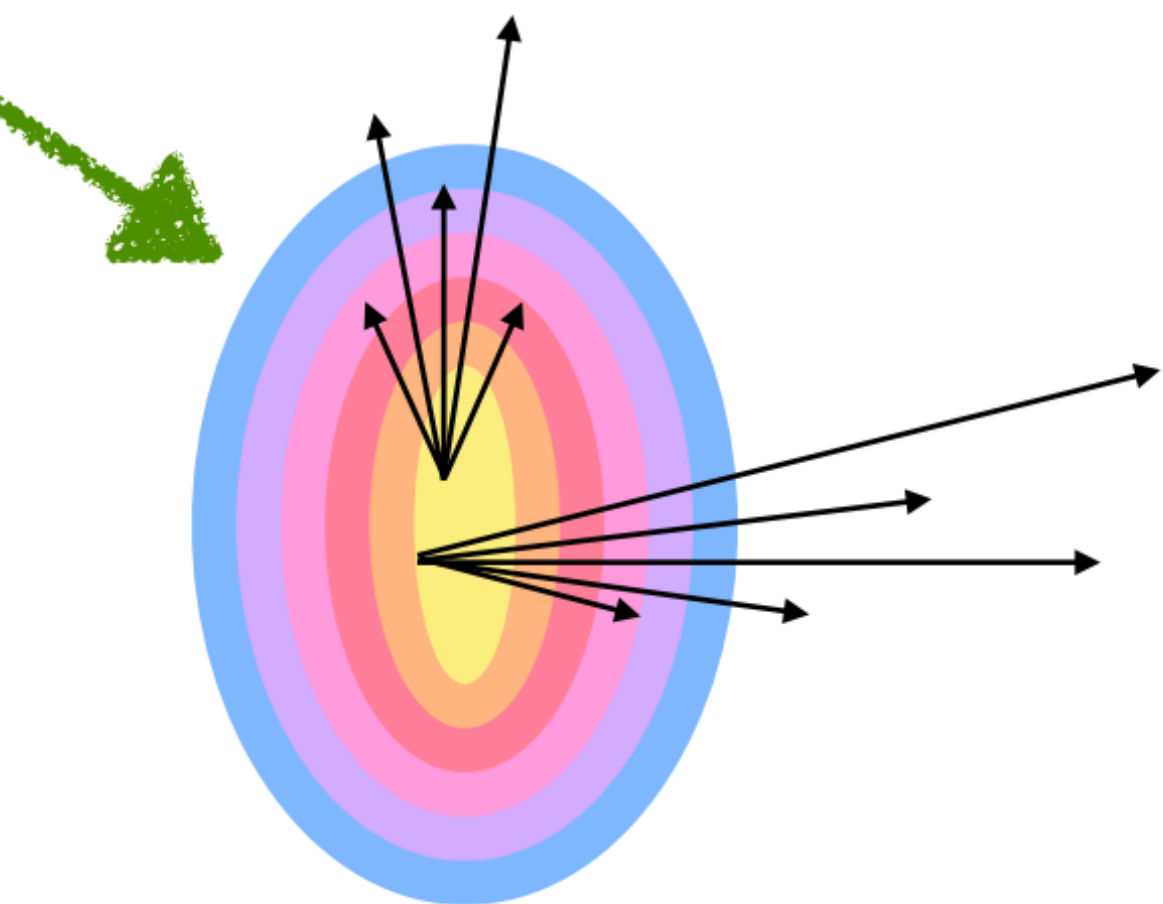
Slide from
K. Hill at QM'19

Hydrodynamics



Transition region

Differential
energy loss



Resummed Quenching Weights

- Use microjet distributions derived using Generating Functional (GF) framework:

Vacuum evol.
obeys DGLAP:

$$\frac{df_{j/i}^{\text{incl}}(z, t)}{dt} = \sum_k \int_z^1 \frac{dz'}{z'} P_{jk}(z') f_{k/i}^{\text{incl}}(z/z', t)$$

Dasgupta et al. - JHEP '14

- Extend GF in the medium to resum energy loss effects due to multi-particle nature of jet:

$$\begin{aligned} \frac{\partial Q_i(p, \theta)}{\partial \ln \theta} &= \int_0^1 dz \frac{\alpha_s(k_\perp)}{2\pi} p_{ji}^{(k)}(z) \Theta_{\text{res}}(z, \theta) \\ &\times [Q_j(zp, \theta)Q_k((1-z)p, \theta) - Q_i(p, \theta)] \end{aligned}$$

PS_{in} constraint

Initial condition at zero angle
is single charge quenching factor:

$$Q_i(p, 0) = Q_{\text{rad}, i}^{(0)}(p_T) Q_{\text{el}, i}^{(0)}(p_T)$$

Radiative
energy loss

Elastic
energy loss

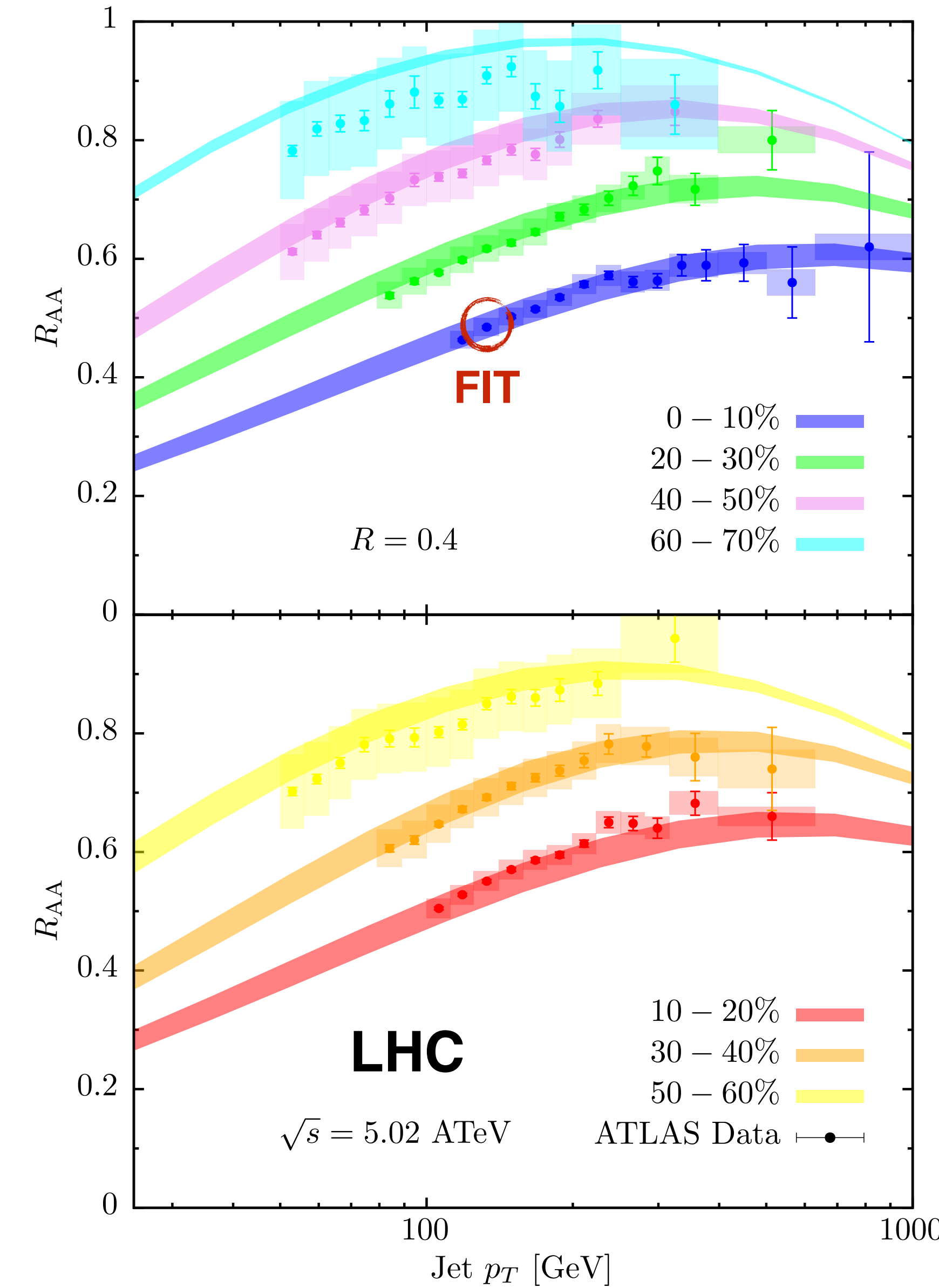
- Energy loss versus R displays non-monotonic behaviour. Competing effects:

- Increasing R means more likely to retain emitted (or thermalised) quanta: **less quenching**.
- Increasing R means larger quenched phase space: **more quenching**.

Mehtar-Tani, DP, Tywoniuk - PRL '21

Jet Suppression at LHC

Mehtar-Tani, DP, Tywoniuk - PRL '21



- Embed framework into realistic heavy-ion environment:
 - Glauber sampling, random azimuthal orientation.
 - Compute event-by-event relevant quantities, e.g.:
 - (in local fluid rest frame)
- $$L = \int_{\Gamma(t)} dx_F \quad \hat{q}_0 \propto \frac{1}{L} \int_{\Gamma(t)} dx_F T^3(x) \left(\frac{p \cdot u(x)}{p^0} \right)$$

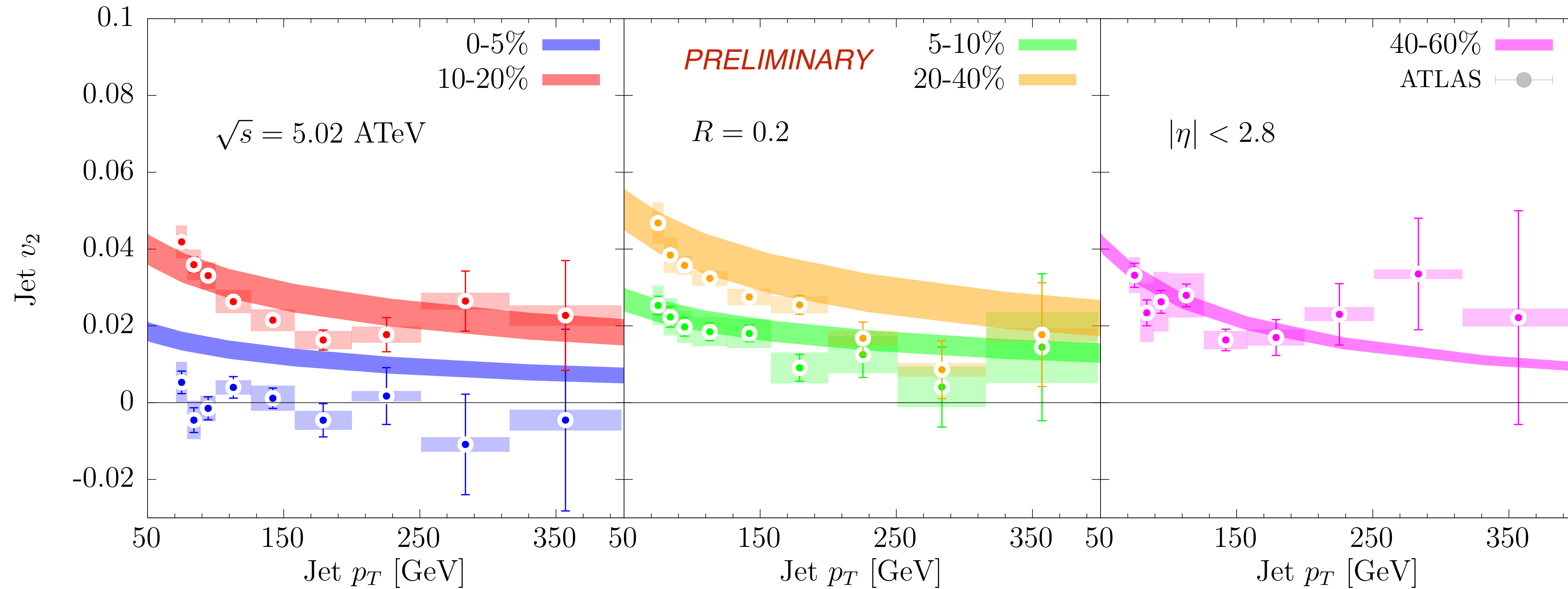
Path of jet through hydro. profile (VISHNU) down to T_c
- g_{med} fit to ATLAS $R=0.4$ around $p_T \sim 120 \text{ GeV}$ at 0-10%
 - $g_{\text{med}} \in \{2.2, 2.3\}$
- $$\langle \hat{q}_0 \rangle \simeq 0.41 \text{ GeV}^2/\text{fm}$$

$$\hat{q} = 2.46 \text{ GeV}^2/\text{fm}$$

due to logarithmic corrections.

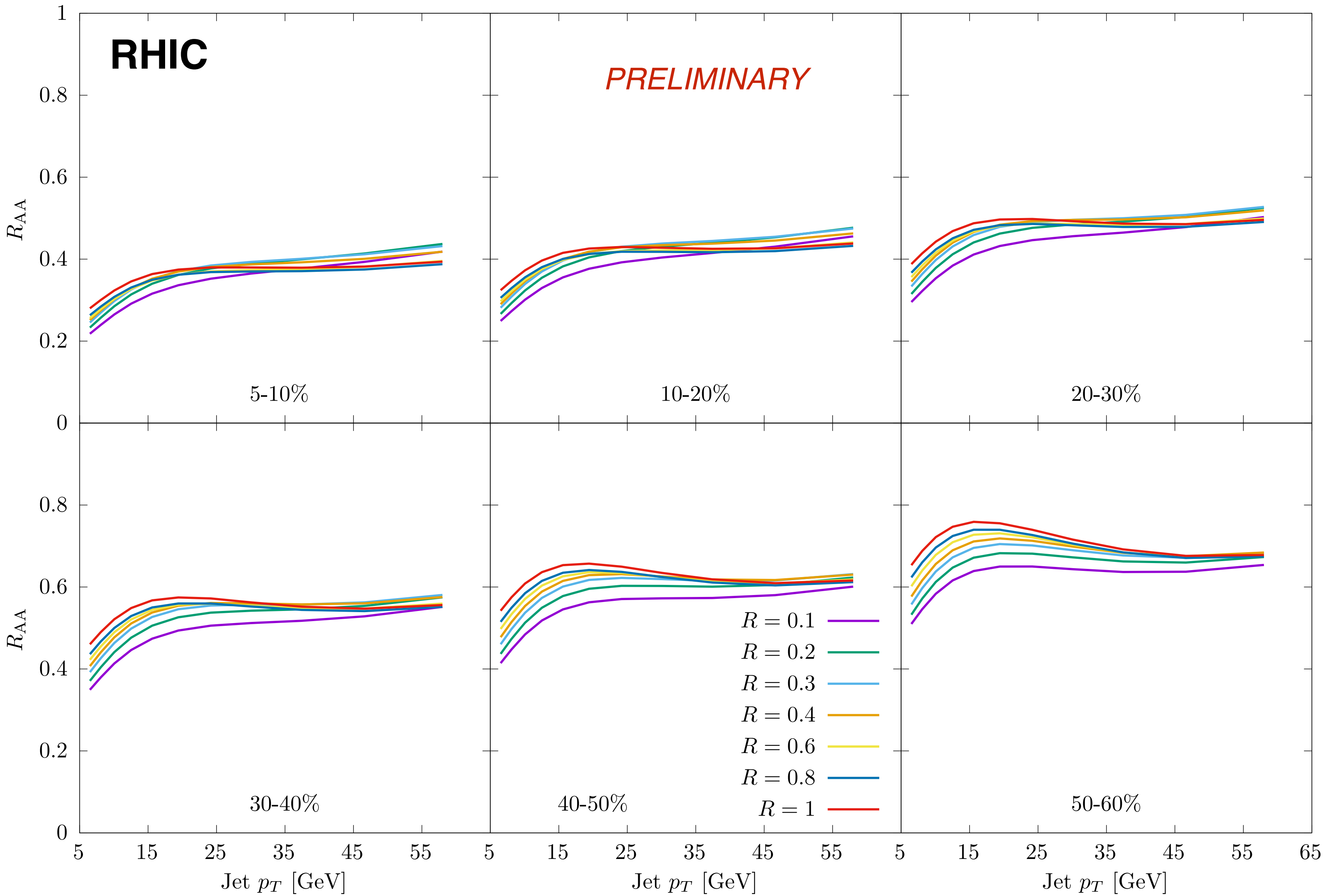
Jet v_2 at LHC for $R=0.2$

Mehtar-Tani, DP, Tywoniuk - in preparation



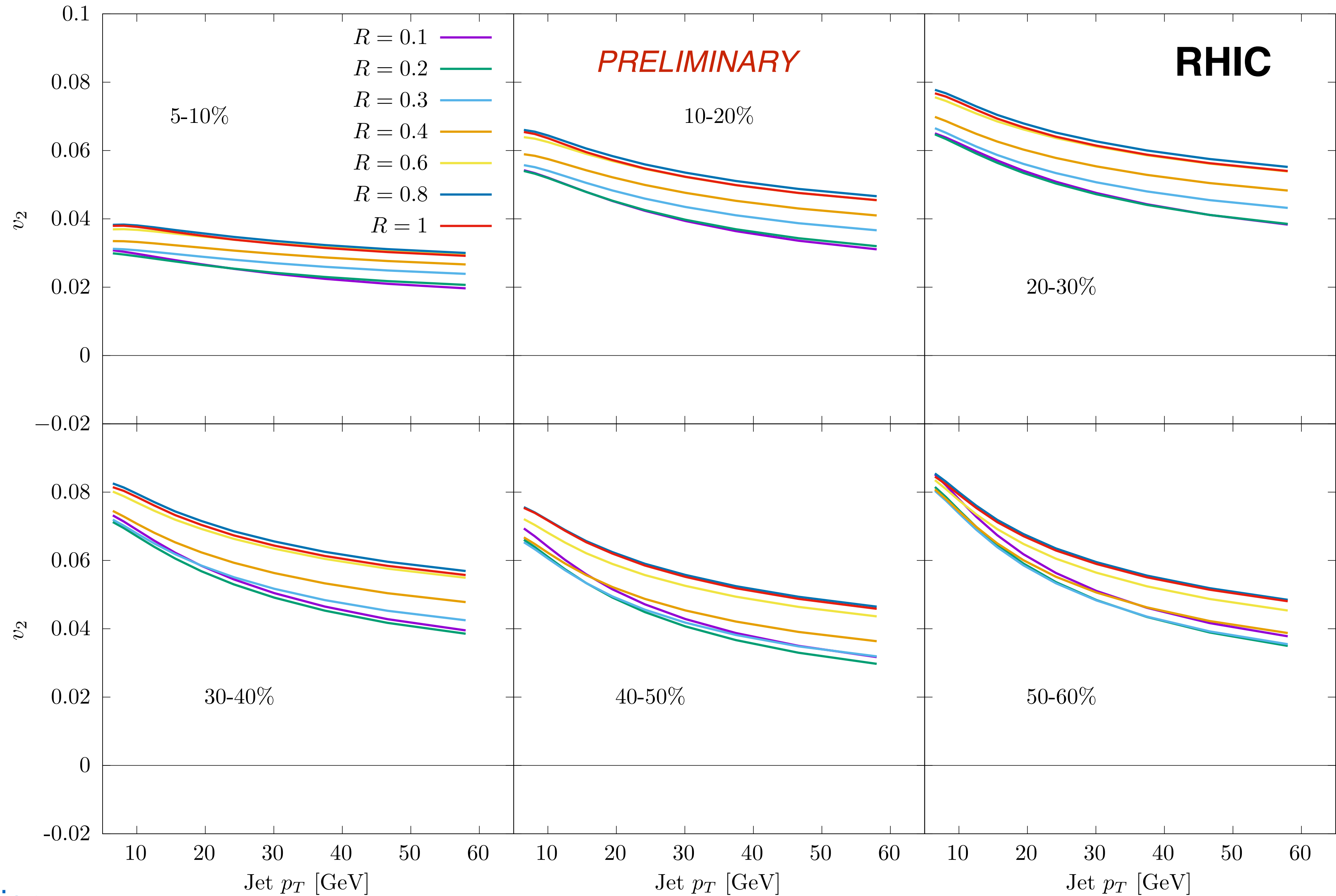
Jet R_{AA} at RHIC

- Even milder R dependence than at LHC.
- In agreement with STAR data.



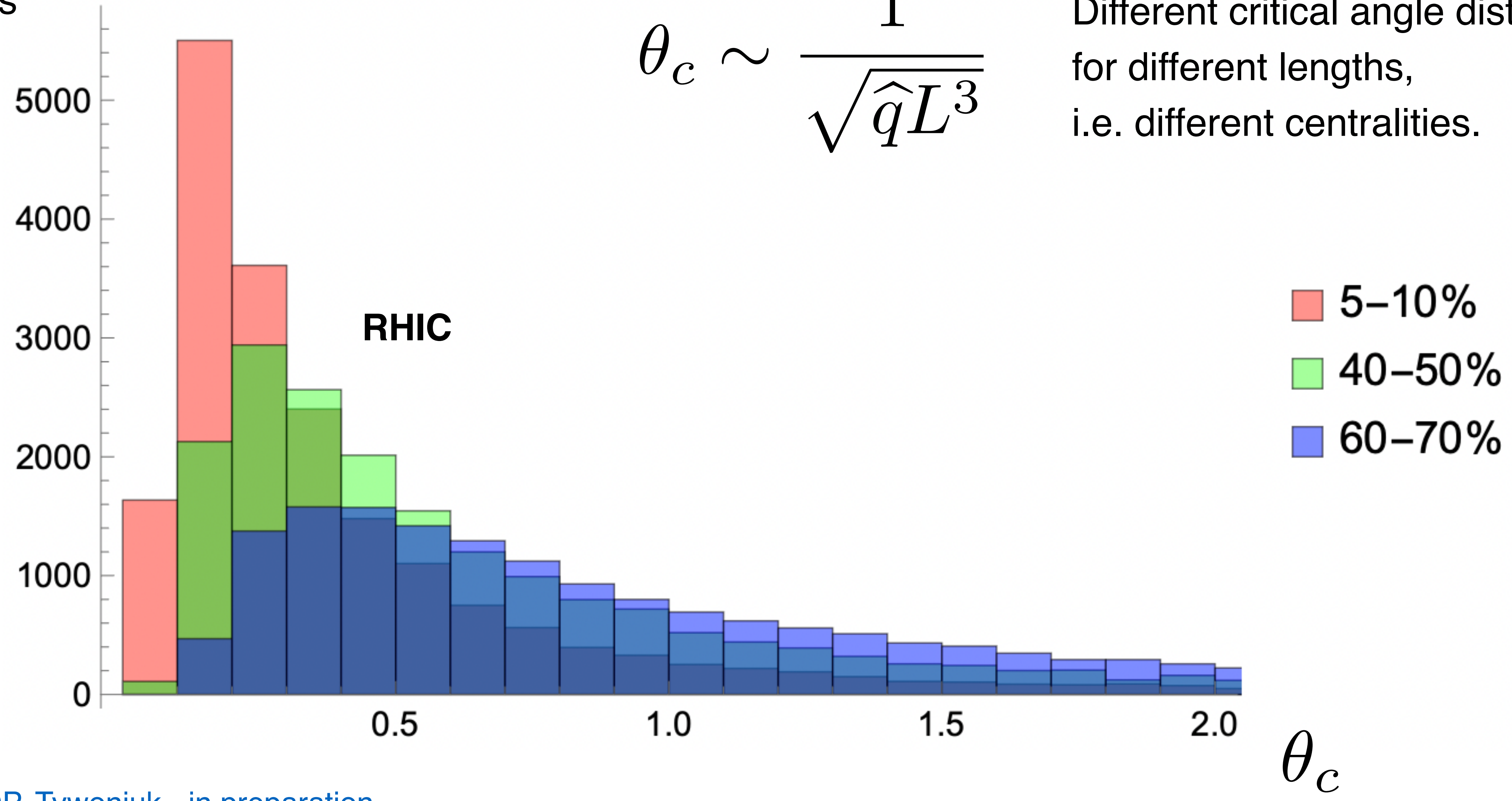
Jet v_2 at RHIC

- Interesting grouping in v_2 for different R .
- $R=0.3$, and especially $R=0.4$, migrate as a function of centrality.

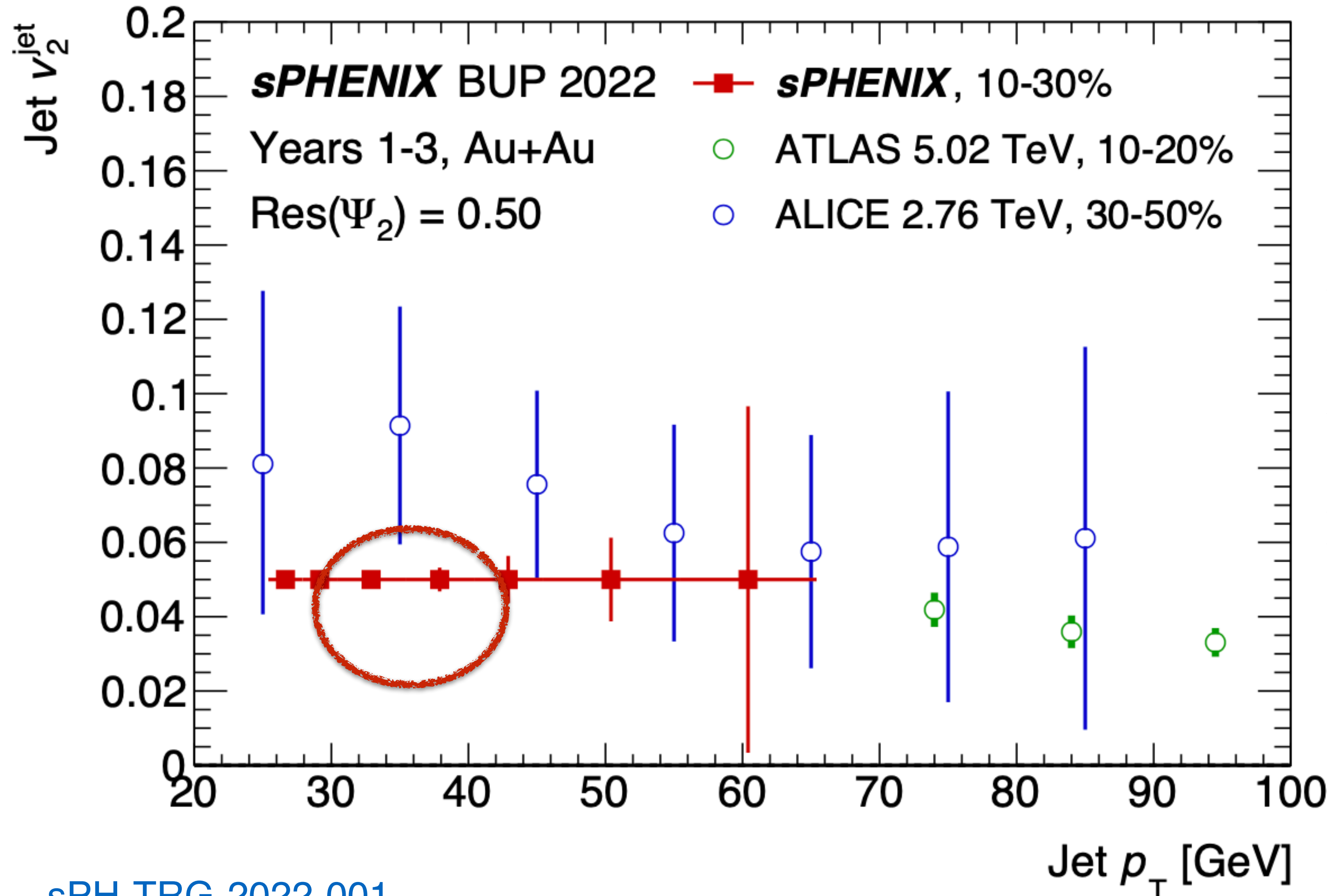


Coherence vs. Centrality

Counts

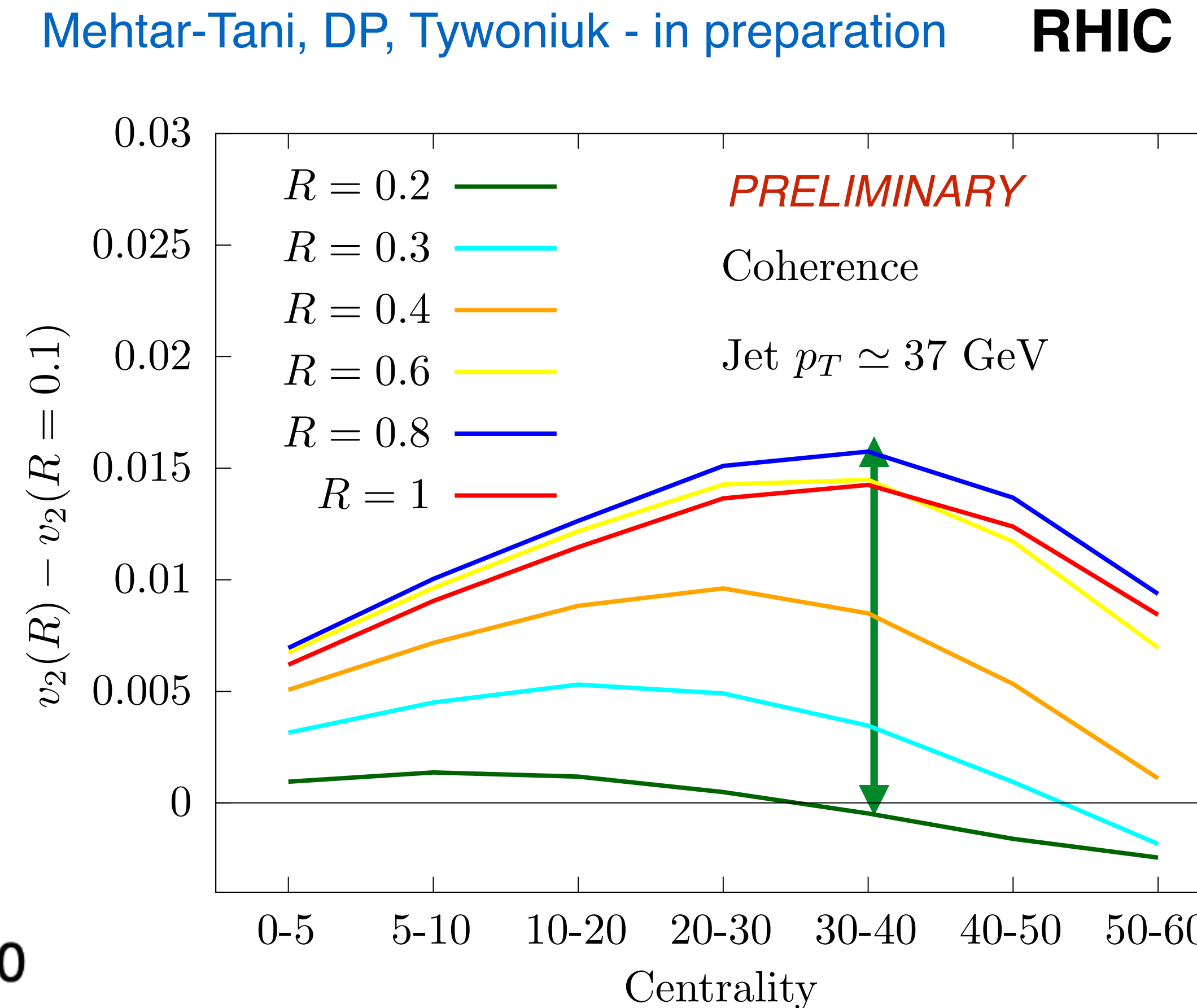


Jet v_2 & Coherence Effects



sPH-TRG-2022-001

Effect can be measured by
sPHENIX.



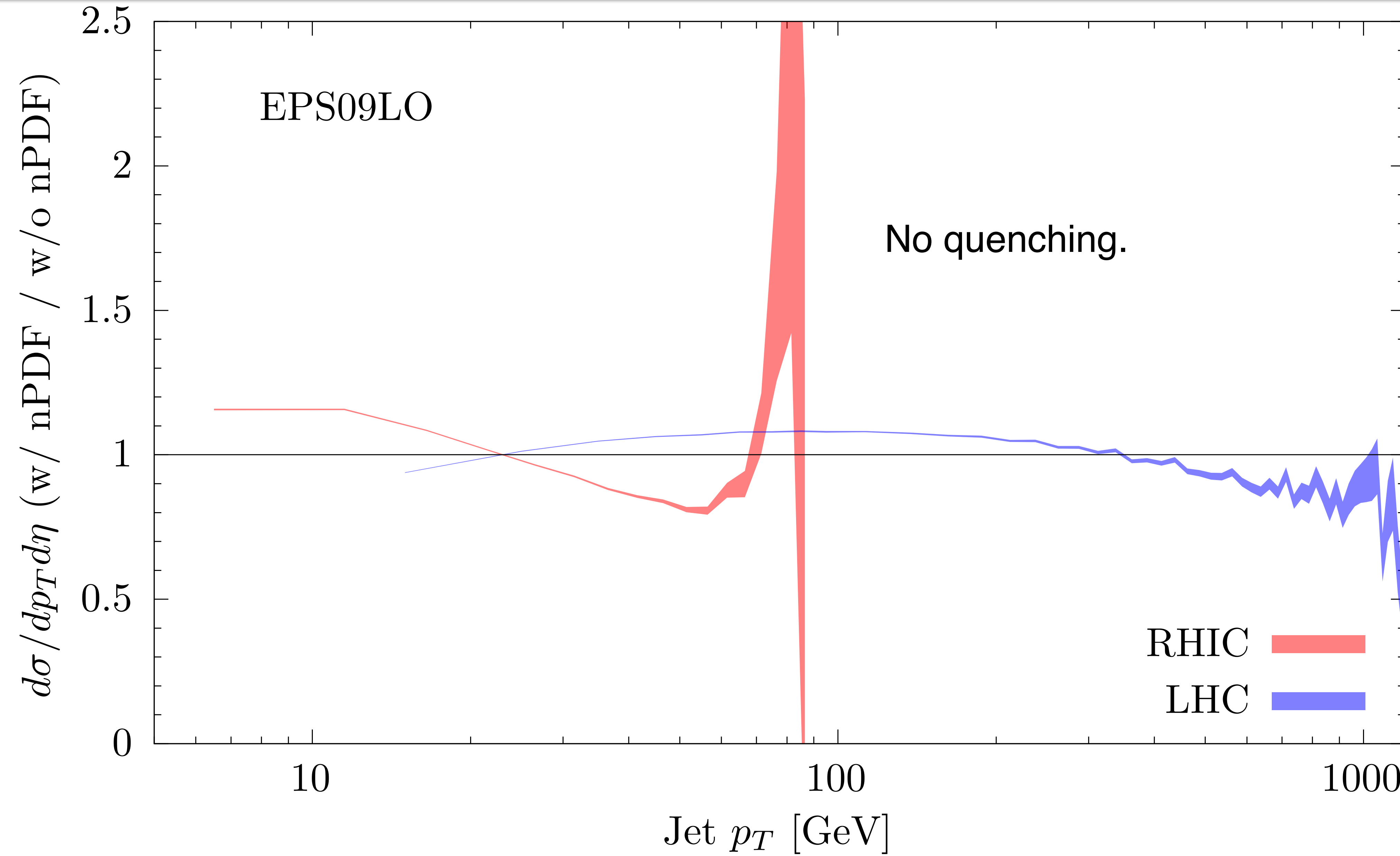
$$\frac{v_2}{e} \approx \begin{cases} 0 & \text{for } R < \theta_c \\ \frac{3\bar{\alpha}}{2} \ln \frac{p_\perp}{\omega_c} (1 - Q_g) & \text{for } R > \theta_c \end{cases}$$

Conclusions

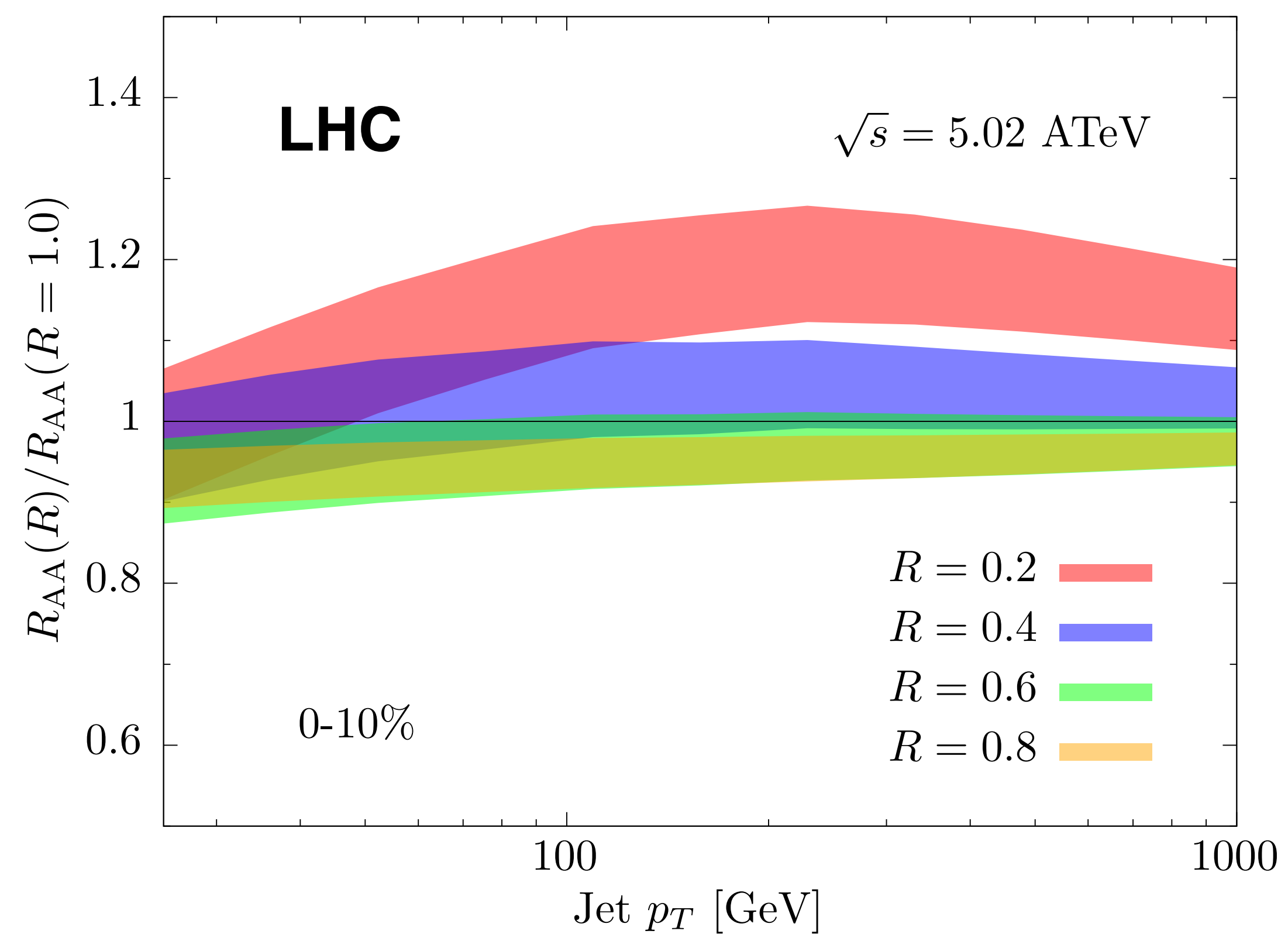
- Jets possess a **narrower substructure** in heavy-ion compared to pp, due to **selection bias**.
 - Wide versus narrow selection bias? **Medium** can **resolve** internal jet scales.
 - Gluon versus quark selection bias? **Medium** does **not** need to **resolve** internal jet scales.
- Use **quark enriched sample** to **disentangle** physical picture. Exploit **rapidity evolution** of q-fraction.
 - If there is still narrowing in quark enriched sample, then medium can resolve jet substructure.
Improved detector acceptance in HL-LHC era.
- Used **leading- k_t** distribution as **proof-of-concept**.
 - No hard radiation or scatterings included. Baseline for future studies.
 - Measurement at LHC in progress.
- R-dependence of jet v_2 is quite sensitive to coherence physics.
 - Average value of critical angle acts as a filter, groups curves into two classes.
 - Motivates measuring R-dependent jet v_2 in future runs at RHIC and LHC.

Backup Slides

Effect of Nuclear PDF



R Dependence & Modelling Uncertainties



Mild R dependence, in agreement with CMS data.

- Modelling sensitivity at $p_T=110$ GeV for R between 0.2 and 0.6:

Parameter	Variation	Effect
θ_c	$[\theta_c/2, 2\theta_c]$	$\lesssim 20\%$
IOE	LO/NLO	$\sim 2\%$
n	± 1	$\sim 10\%$
R_{rec}	$[1, \infty]$	$\sqrt{\sim} 10\%$
ω_s	$[\omega_s/2, 2\omega_s]$	$\sqrt{\sim} 8\%$

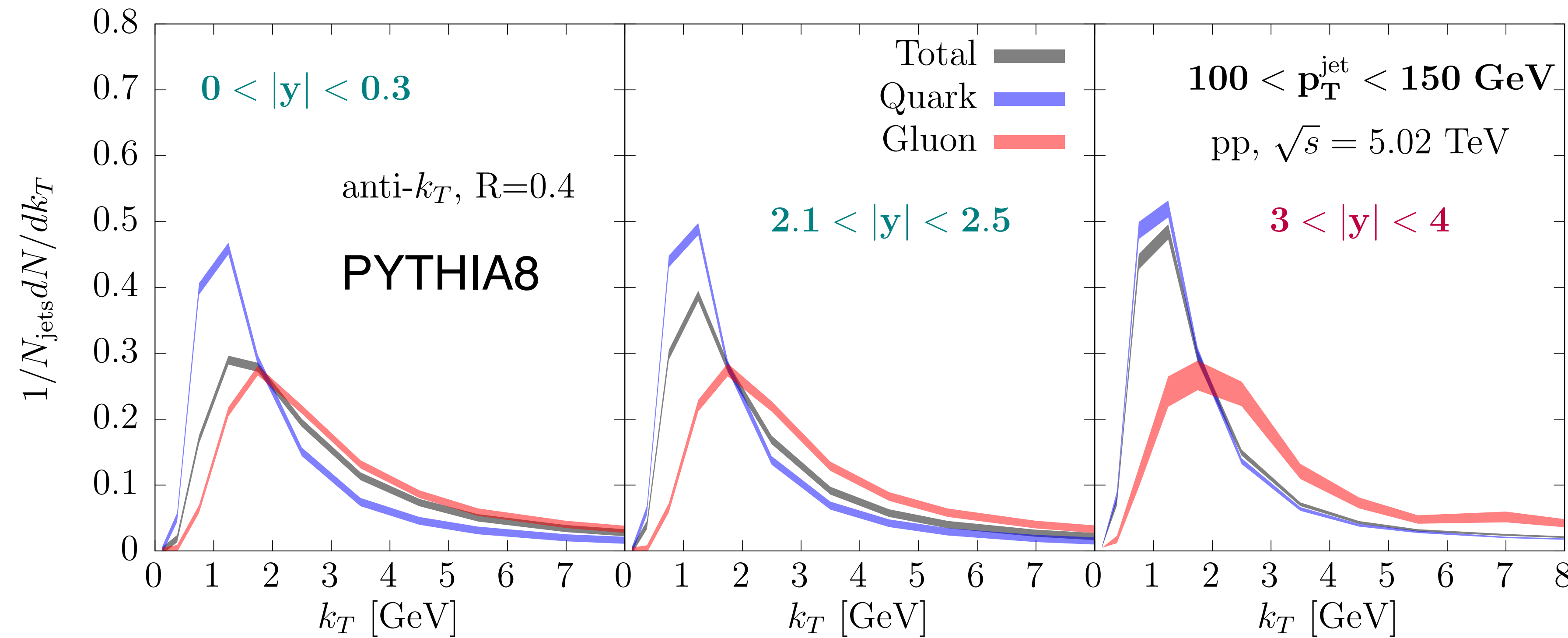
- NLO contribution very small
(hard emissions tend to be collinear).
- Modelling of fate of lost energy relatively small.
- Determination of quenched phase space
relatively large. Improvable in pQCD.

Need to improve perturbative sector before
non-perturbative becomes relevant (for $R < 0.6$!)

Leading- k_T Distribution in pp

$$k_t \equiv z p_t^{\text{parent}} \sin \theta$$

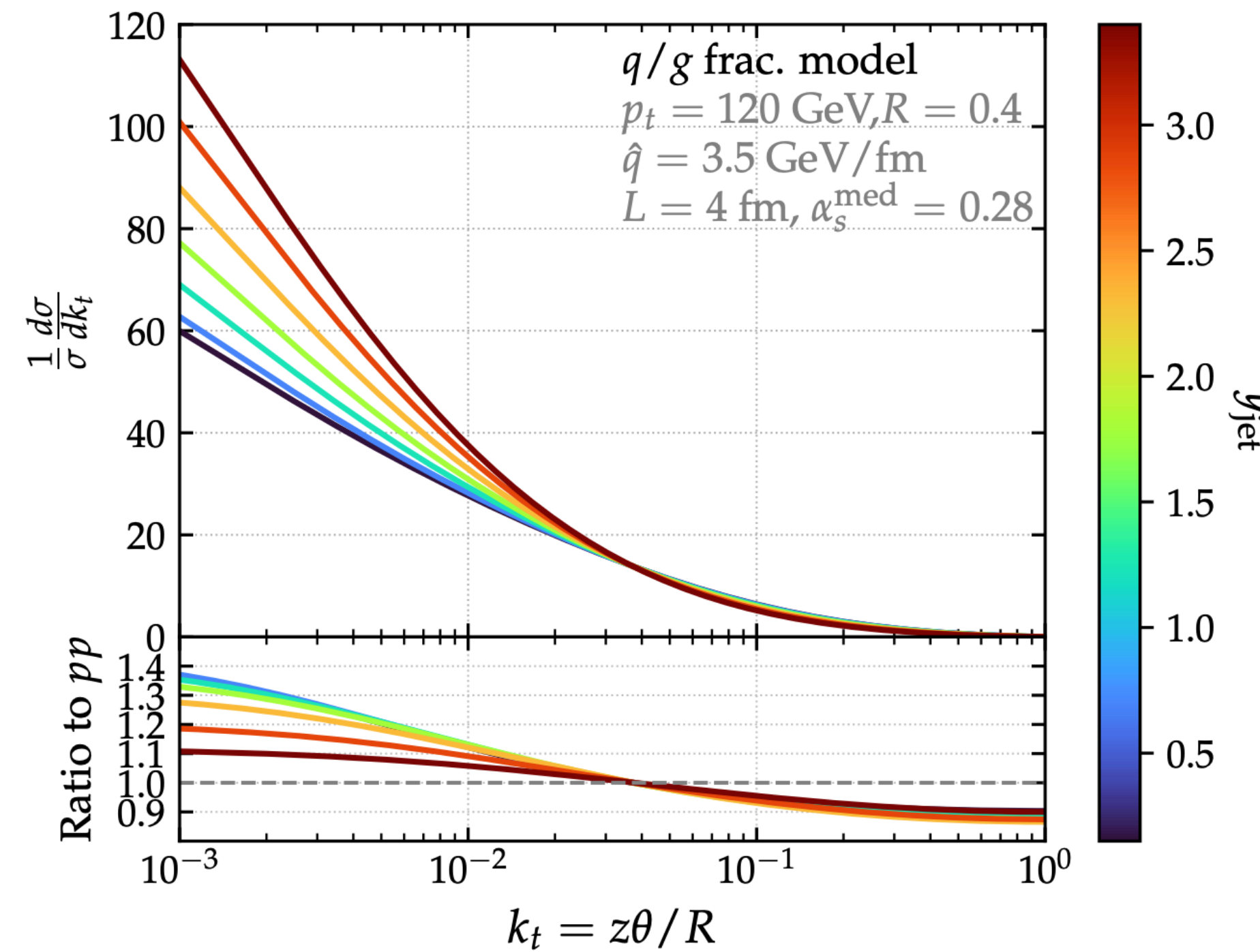
DP & A. Soto-Ontoso - 2210.07901



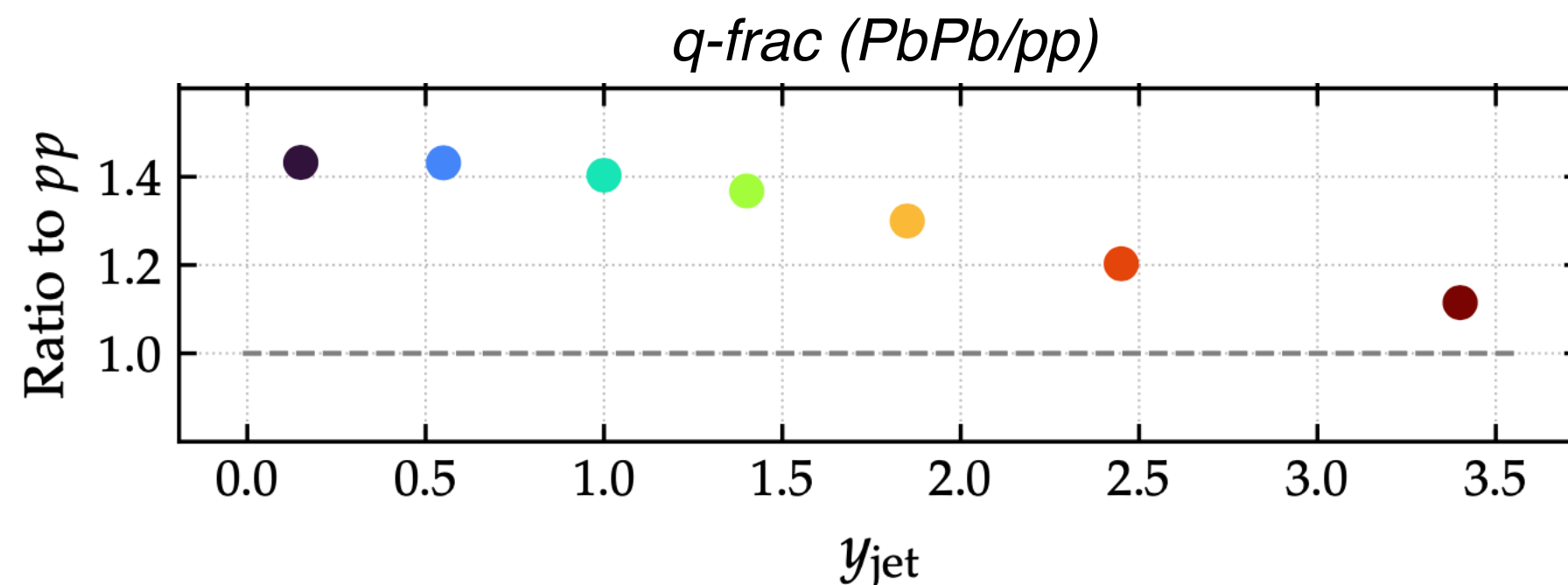
- Compute leading- k_t in a C/A reclustered tree.
- Distribution for quark jets narrower than for gluon jets.
- Moving to forward rapidities, sample dominated by quark jets.

Analytic q/g frac. model at DLA

DP & A. Soto-Ontoso - 2210.07901



Less narrowing with increasing rapidity.



(Note: effect at mid-rapidity not as big as Ringer et al., different medium q/g fraction).

nPDF-modified q/g fractions (small effect)

$$\frac{1}{\sigma} \frac{d\sigma}{dk_t} \Big|_{p_t, y} = \frac{1}{N} \sum_{i \in \{q, g\}} \boxed{f_i^n} \int_0^1 dz \int_0^R d\theta P_i^{\text{med}}(z, \theta) \\ \times e^{- \int dz' \int d\theta' P^{\text{med}}(z', \theta') \Theta(z'\theta' - k_t) \delta(k_t - z\theta)} \\ \times \boxed{\int_0^\infty d\varepsilon \mathcal{E}_i(\varepsilon | z, \theta) e^{-\frac{n\varepsilon}{p_t}}}$$

q/g frac model:

Triggered splitting assumed vacuum-like only.

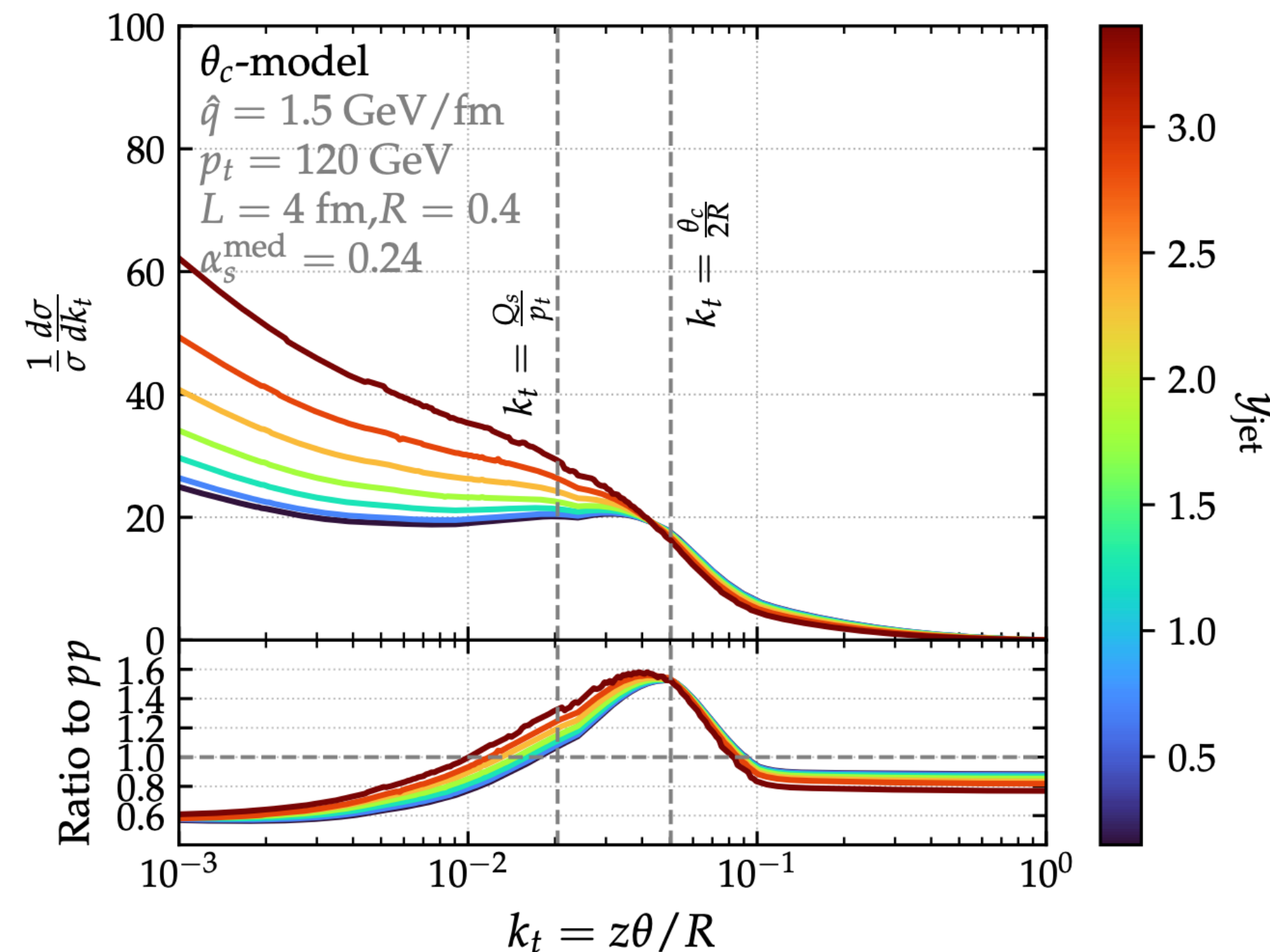
→ $P^{\text{med}} \rightarrow \bar{\alpha}/(z\theta)$

Quenching of leading charge only.

→ $Q_i(p_t, R) \equiv \int_0^\infty d\varepsilon \mathcal{E}_i(\varepsilon | z, \theta) e^{-\frac{n\varepsilon}{p_t}}$

Analytic decoherence model at DLA

DP & A. Soto-Ontoso - 2210.07901



Narrowing persists also at forward rapidities.

nPDF-modified q/g fractions (small effect)

$$\frac{1}{\sigma} \left. \frac{d\sigma}{dk_t} \right|_{p_t, y} = \frac{1}{N} \sum_{i \in \{q, g\}} \boxed{f_i^n} \int_0^1 dz \int_0^R d\theta P_i^{\text{med}}(z, \theta) \\ \times e^{- \int dz' \int d\theta' P^{\text{med}}(z', \theta') \Theta(z'\theta' - k_t) \delta(k_t - z\theta)} \\ \times \boxed{\int_0^\infty d\varepsilon \mathcal{E}_i(\varepsilon | z, \theta) e^{-\frac{n\varepsilon}{p_t}}}$$

θ_c model:

Triggered splitting can be medium-induced.

→ $P^{\text{med}}(z, \theta) = P^{\text{vac}}(z, \theta) \Theta_{\notin \text{veto}}(z, \theta) + P^{\text{mie}}(z, \theta)$

Quenching of leading and tagged prongs if resolved (i.e. with $\theta > \theta_c$).

→ $\int_0^\infty d\varepsilon \mathcal{E}_i(\varepsilon | z, \theta) e^{-\frac{n\varepsilon}{p_t}} = (1 - \Theta_{\text{res}}) Q_i(p_t, R)$

$$\Theta_{\text{res}}(z, \theta) = \Theta(\theta - \theta_c) \Theta(k_t - k_{t,\text{med}}) + \Theta_{\text{res}} Q_g(p_t, R) Q_i(p_t, R)$$

Hybrid Strong/Weak Coupling Model

$$\frac{1}{E_{\text{in}}} \frac{dE}{dx} = -\frac{4}{\pi} \frac{x^2}{x_{\text{stop}}^2} \frac{1}{\sqrt{x_{\text{stop}}^2 - x^2}}$$

$$x_{\text{stop}} = \frac{1}{2} \frac{E_{\text{in}}^{1/3}}{\kappa_{\text{sc}} T^{4/3}}$$

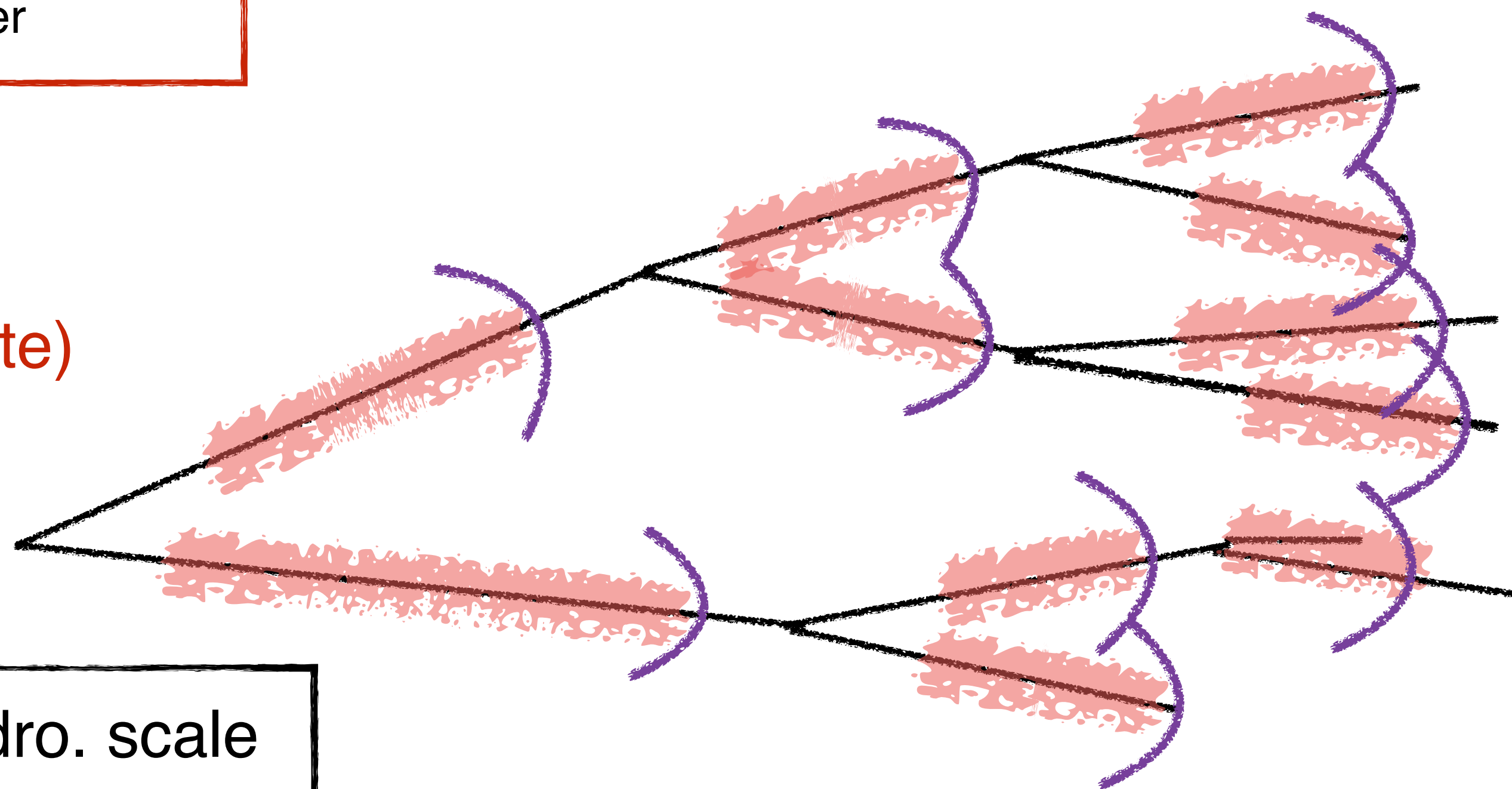
$\mathcal{O}(1)$ free parameter

Strongly coupled
energy loss
(hydrodynamization rate)

$$E \frac{d\Delta N}{d^3p} = \frac{1}{32\pi} \frac{m_T}{T^5} \cosh(y - y_j) \exp \left[-\frac{m_T}{T} \cosh(y - y_j) \right]$$

$$\left\{ p_T \Delta P_T \cos(\phi - \phi_j) + \frac{1}{3} m_T \Delta M_T \cosh(y - y_j) \right\}$$

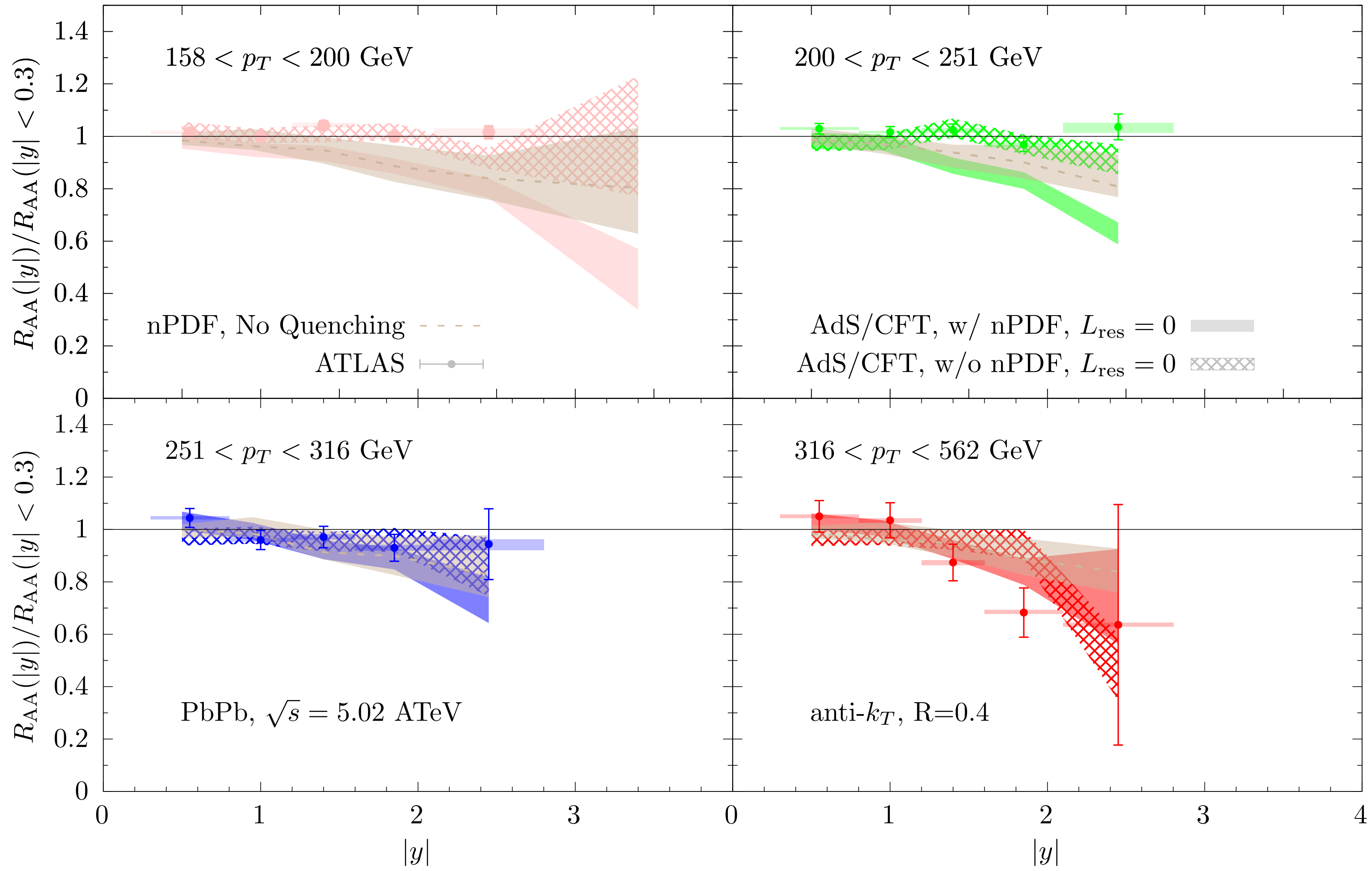
Hadrons from the hydro.
wake (medium response)



PYTHIA8 down to hadro. scale
(formation time argument
for spacetime picture)

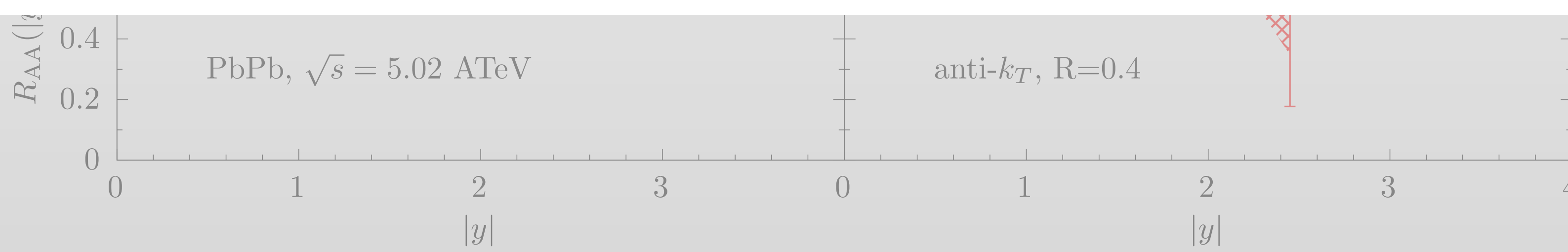
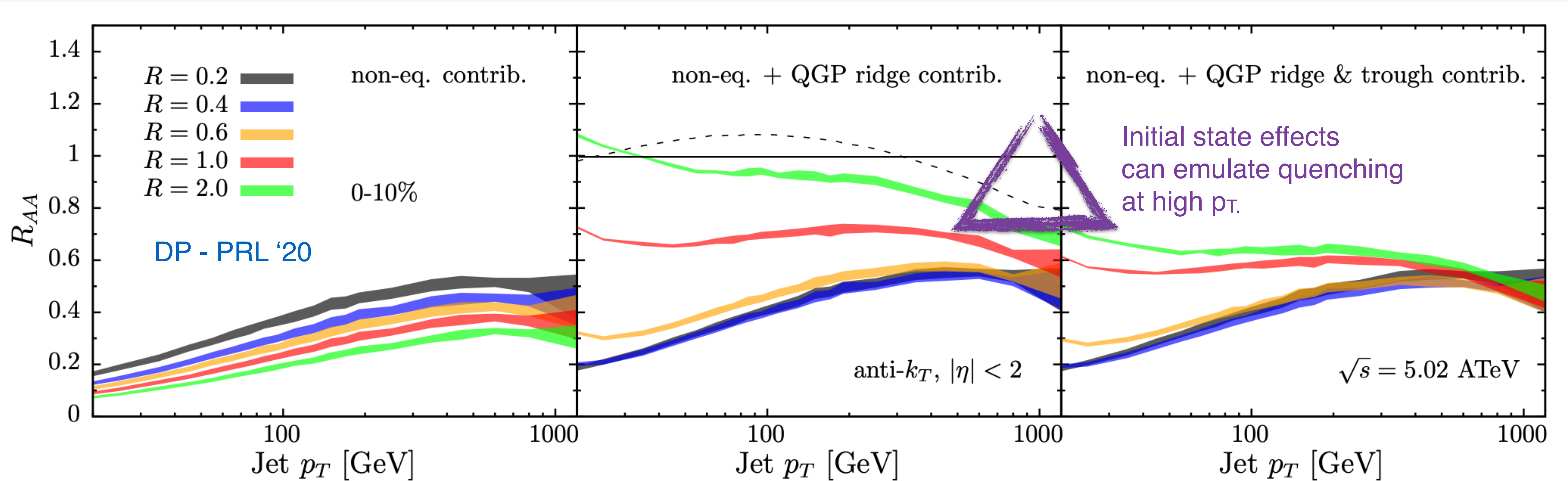
Casalderrey-Solana, Gulhan,
Milhano, DP,
Rajagopal JHEP '15, '16, '17

Rapidity Depence of R_{AA}



- Without nPDF, flatness of R_{AA} result of competing effects:
Steepness of spectrum, change in q-fraction.
- Initial state effects affect R_{AA} vs rapidity.
(Also observed in Adhya et al. - EPJC '22.)
- Need to check with updated sets EPPS21 and nNNPDF3.0.
Differences among nPDF?
Could we constrain nPDF?

Rapidity Depence of R_{AA}



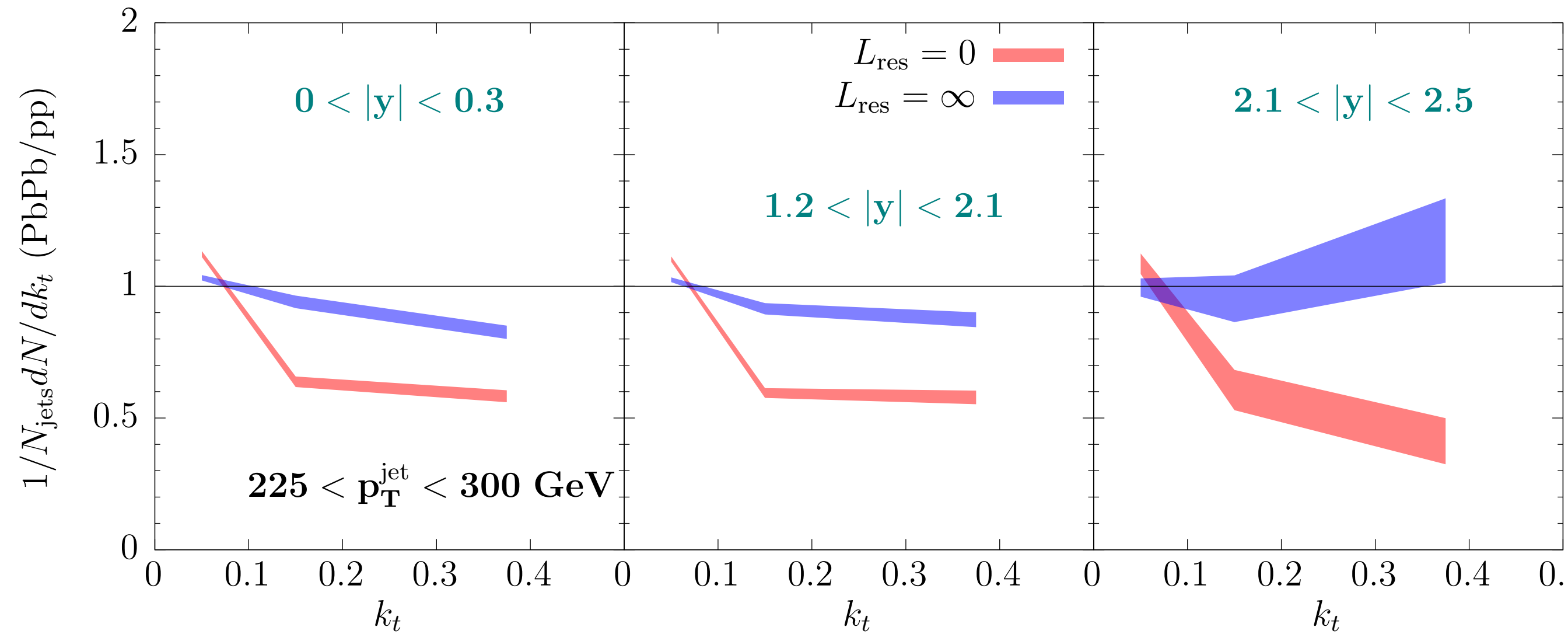
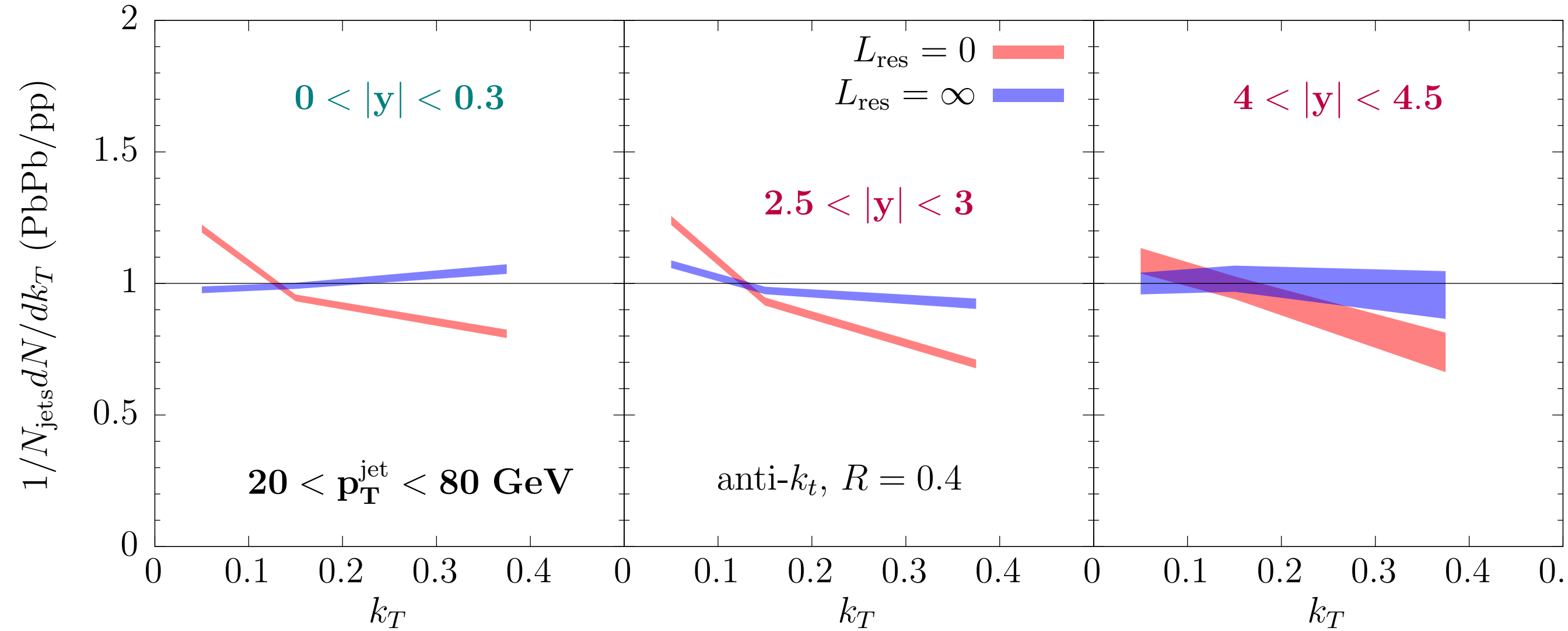
- Need to use updated sets EPPS21 and nNNPDF3.0.
- Differences?
- Could we constrain?

Hybrid Model

0-5% Centrality

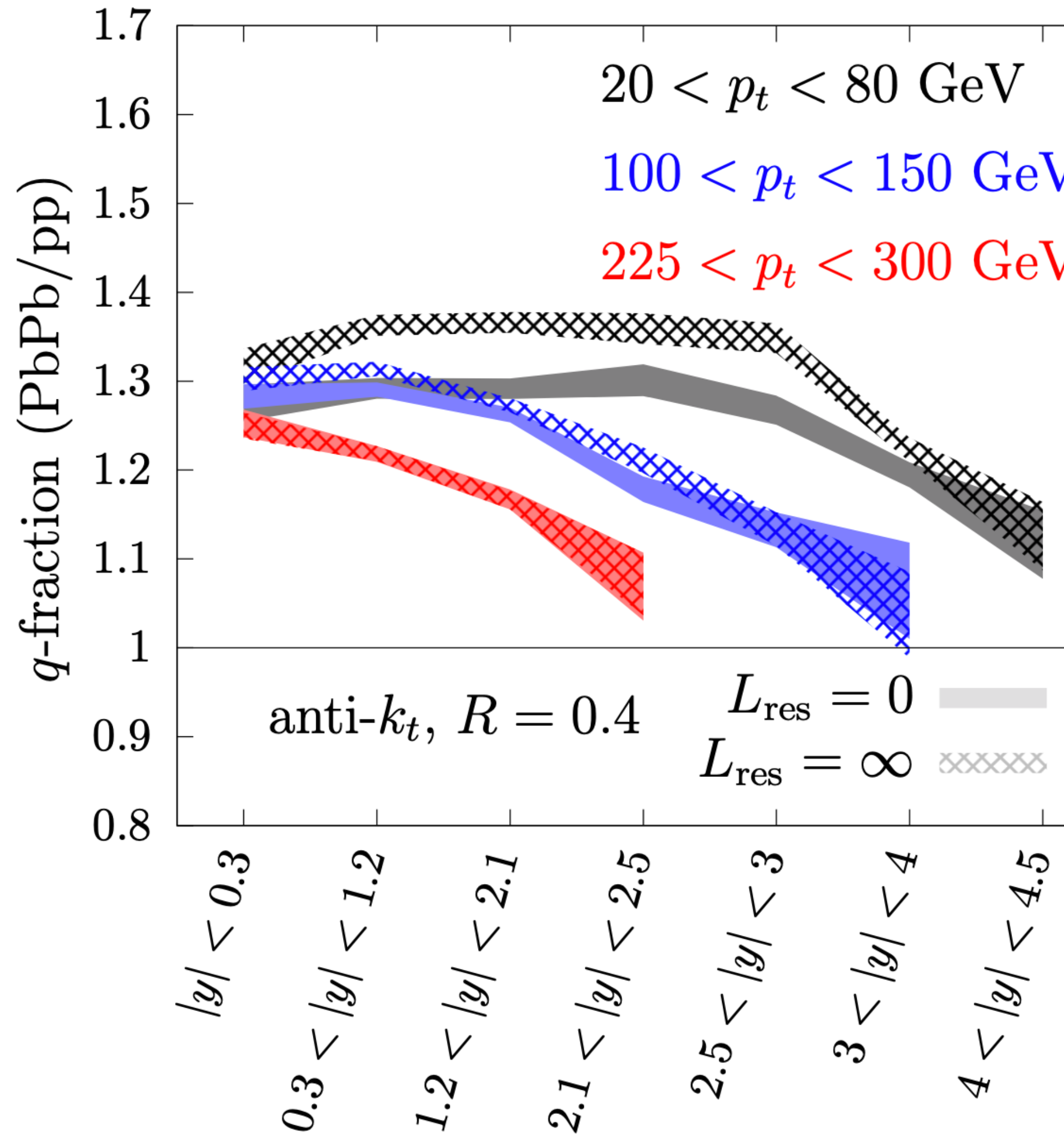
Using statistics projected for HL-LHC

$$k_t \equiv z(p_t^{\text{parent}}/p_t^{\text{jet}}) \sin \theta / R$$



- Wake affects substructure of low p_T jets.
- At high rapidity, q-fraction evolves strongly with p_T .
- Increasing rapidity can make distribution narrower due to jet p_T -bin migration
- At high-enough p_T , current detectors' acceptance suffices to get high q-fraction.

q-fraction in the Hybrid Model



- At low p_T , q-fraction increases if sensitive to total color charge only.
- At high p_T , differences disappear.
- q-fraction ratio (PbPb/pp) in small e-loss approx:

$$f_q^{\text{ratio}} \approx 1 + (1 - f_q)(\varepsilon_g - \varepsilon_q) \frac{n}{p_t} + \mathcal{O}((\varepsilon n/p_t)^2)$$

Collimator in linearised approx:

Mehtar-Tani, Tywoniuk - PRD '18

$$\varepsilon_q \sim C_F \hat{\varepsilon} [1 + C_A \mathcal{A}(p_t, R)],$$

$$\varepsilon_g \sim C_A \hat{\varepsilon} [1 + C_A \mathcal{A}(p_t, R)]$$

$$\mathcal{A}_0 = \frac{\alpha_s}{\pi} \int \frac{dz}{z} \int \frac{d\theta}{\theta} \Theta(t_f < L) \Theta(\theta < R)$$

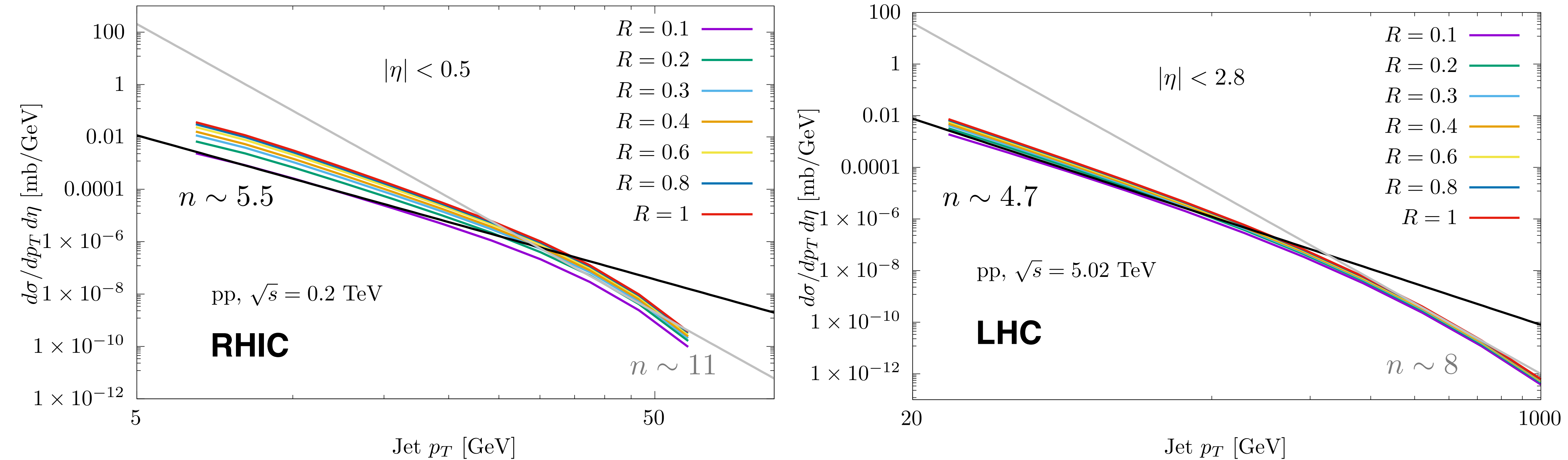
$$= \frac{\alpha_s}{4\pi} \ln^2 \left(\frac{p_t R^2 L}{2} \right),$$

$\mathcal{A}(p_t, R)$
is phase-space
of extra energy loss
sources.

$$\mathcal{A}_\infty \rightarrow 0$$

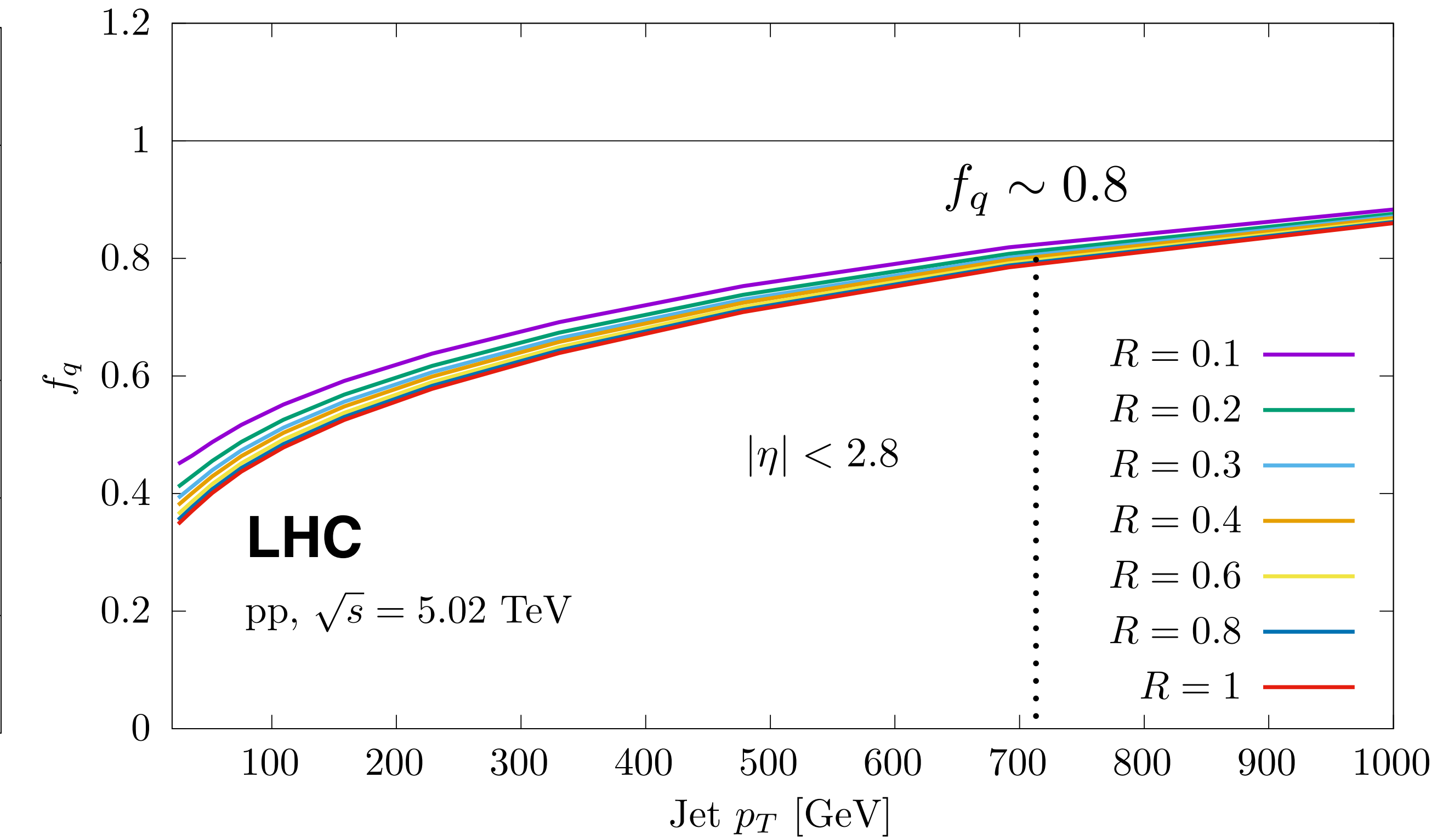
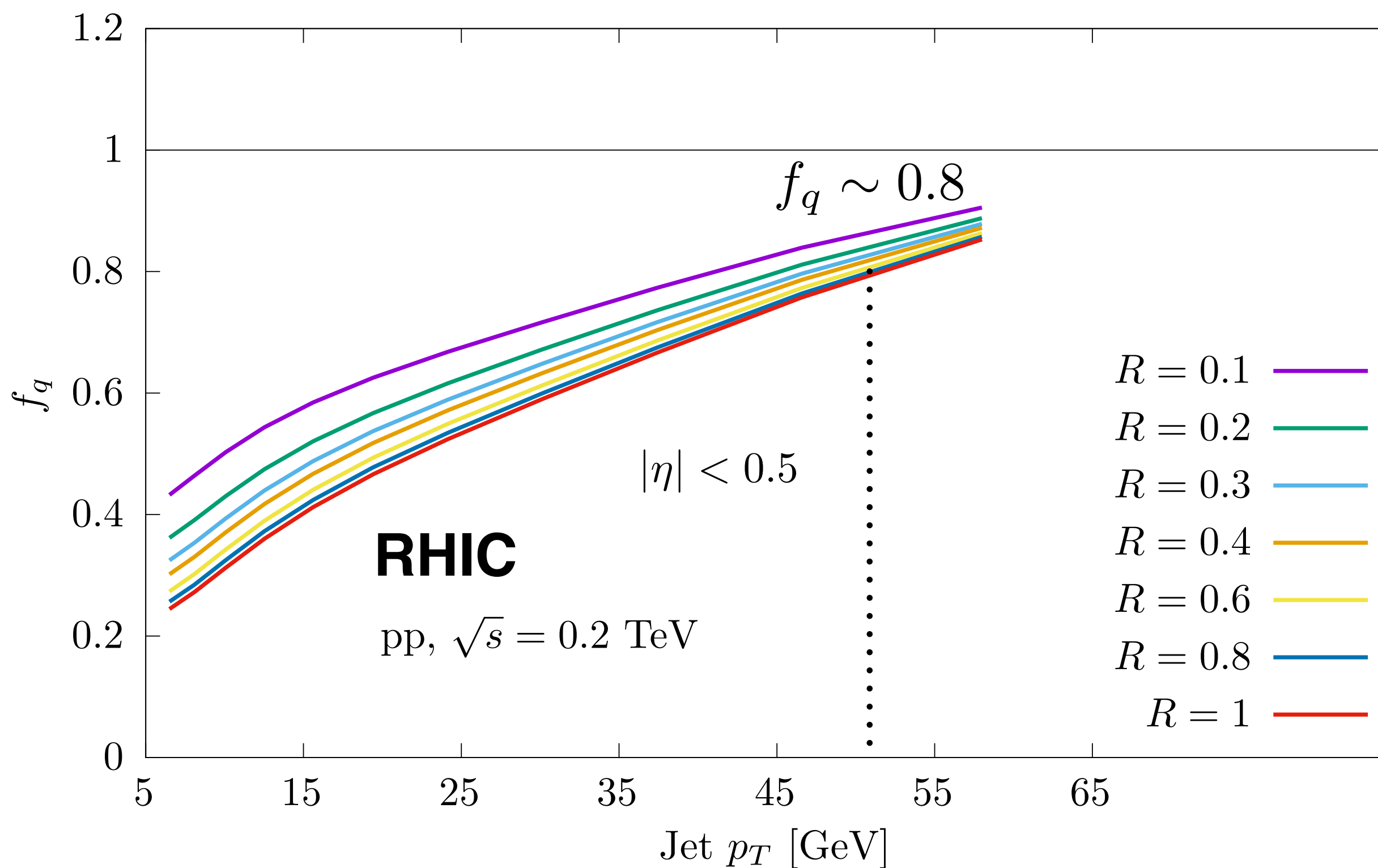
→ Explains behaviour in MC.

RHIC vs LHC Vacuum Spectra



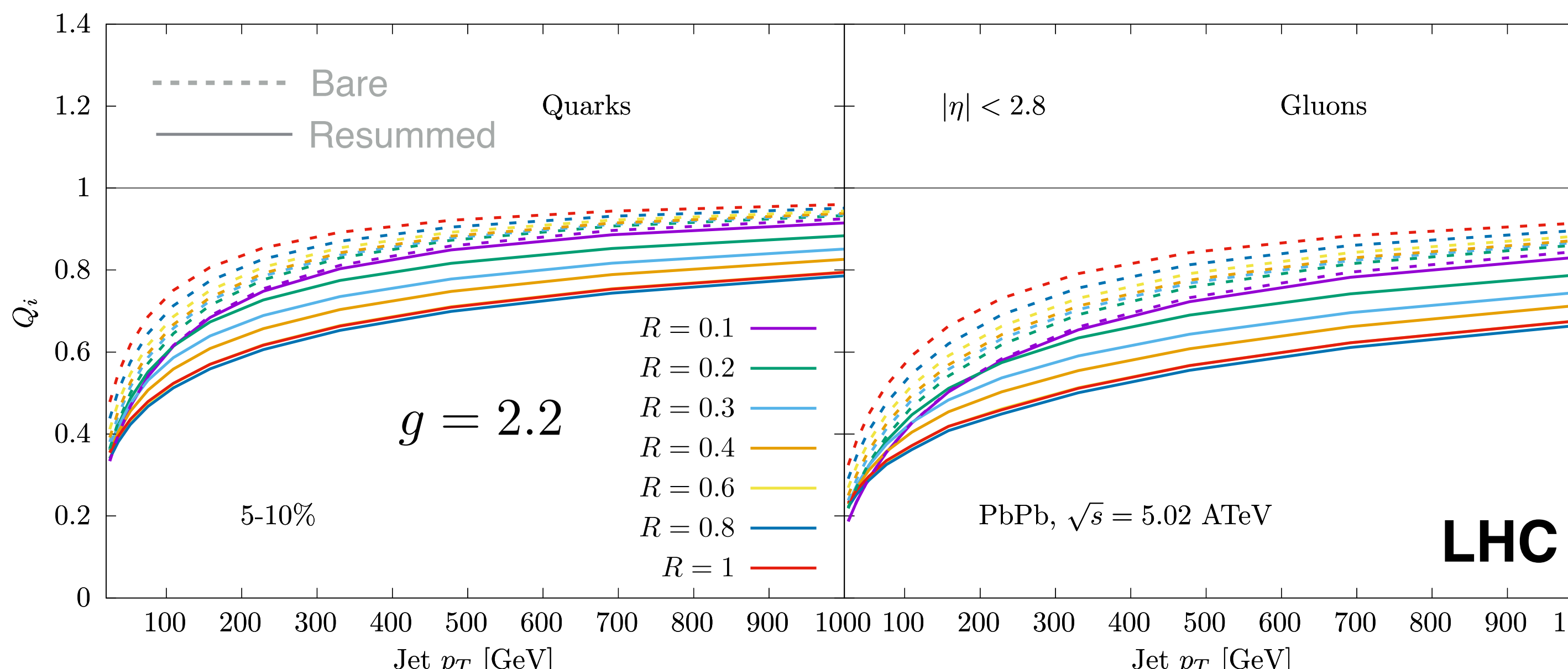
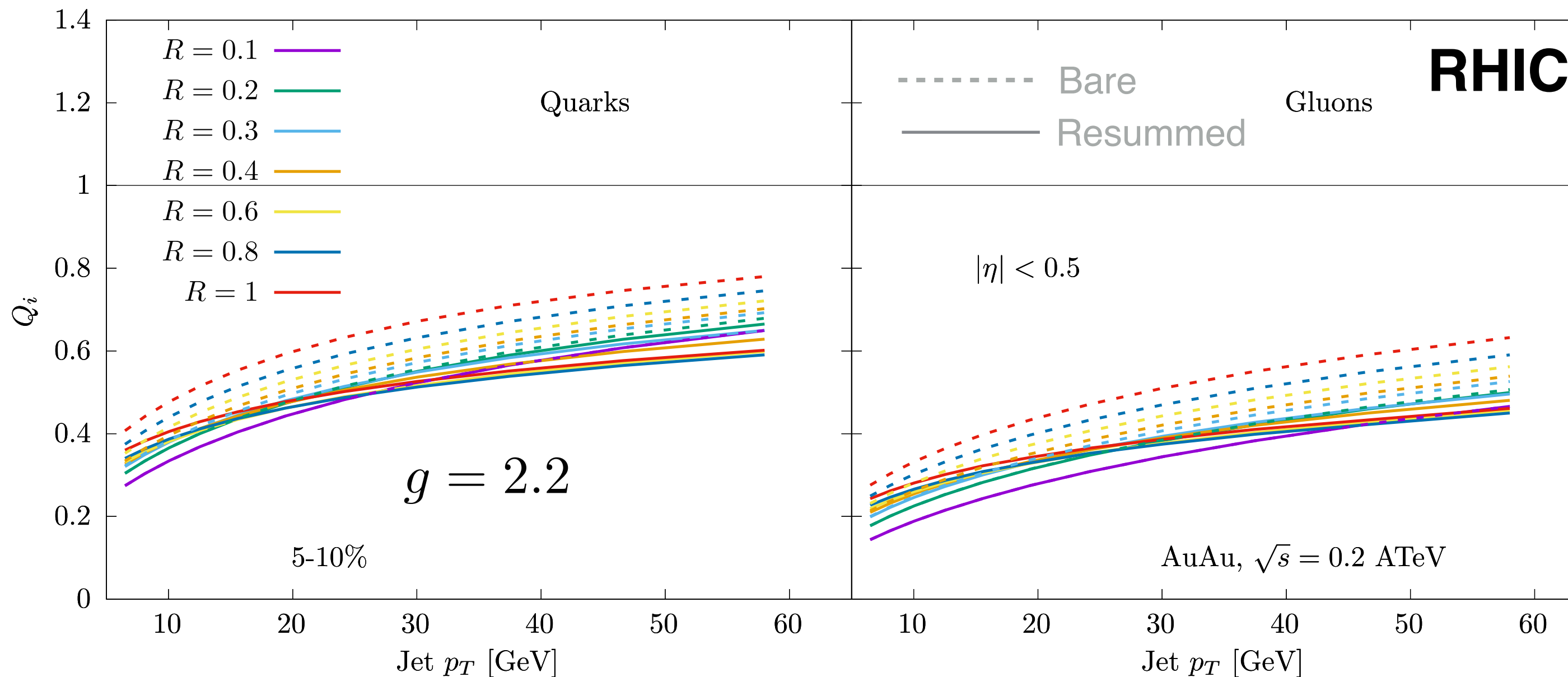
- Spectra increases with increasing R due to recapturing out-of-cone radiation.
- Steeper spectrum at RHIC energies, will push R_{AA} down.

RHIC vs LHC Vacuum Quark Fraction

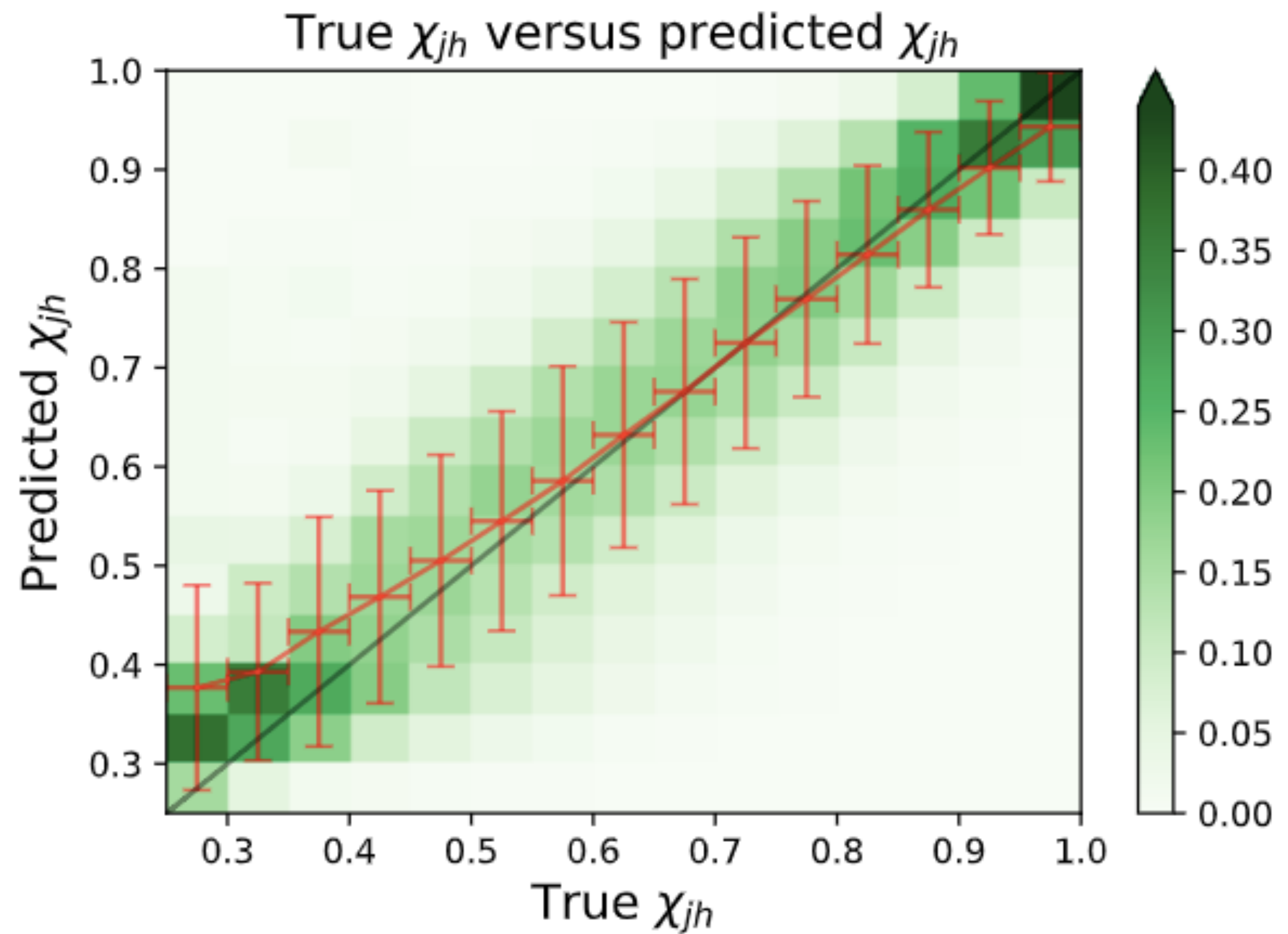
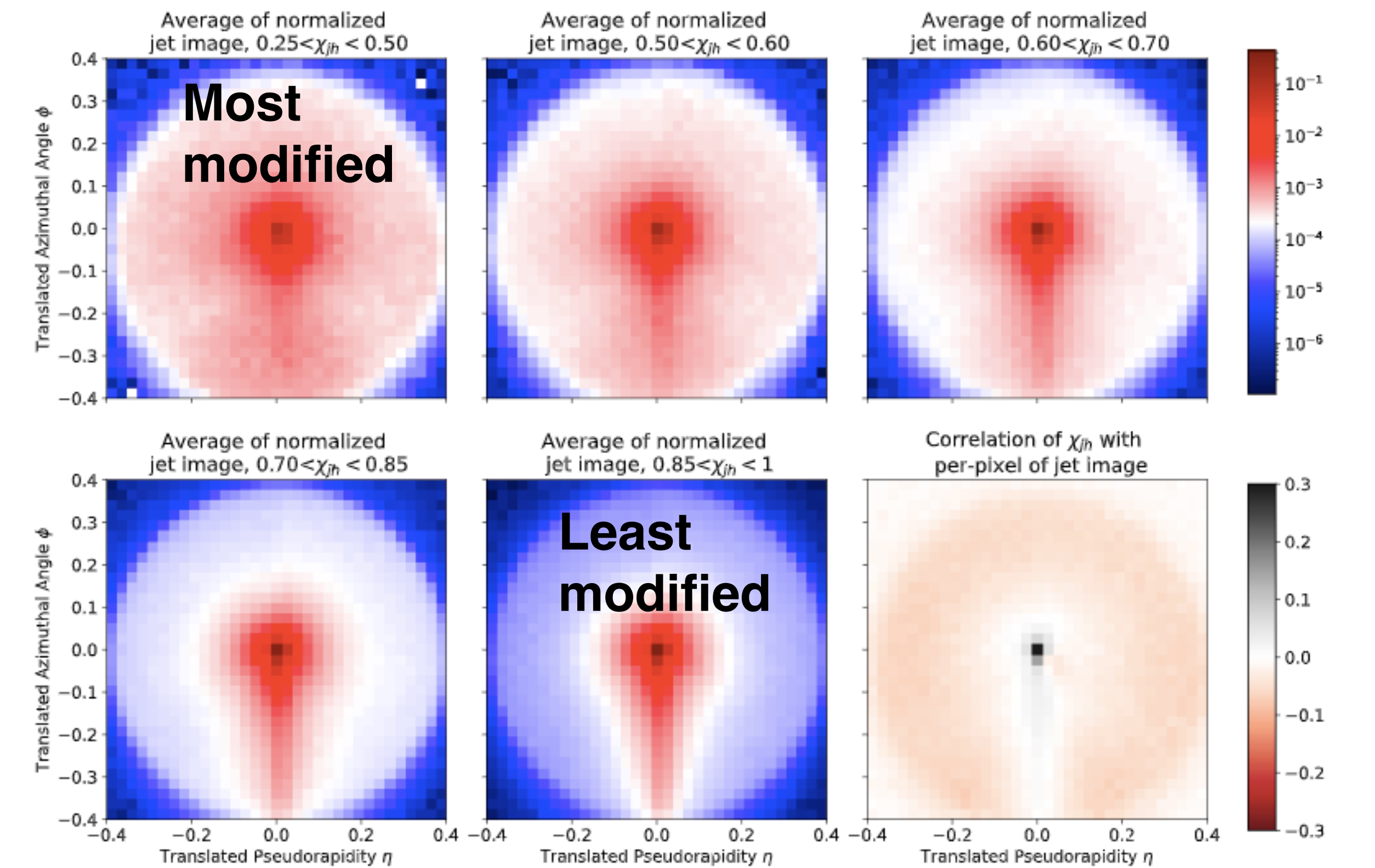


- Quark-initiated jet fraction decreases with increasing R , as gluon-initiated jets are more active.
- Larger quark-initiated jet fraction at RHIC, should push total R_{AA} up.

RHIC vs LHC Quenching Factor



Deep Learning Jet Modifications

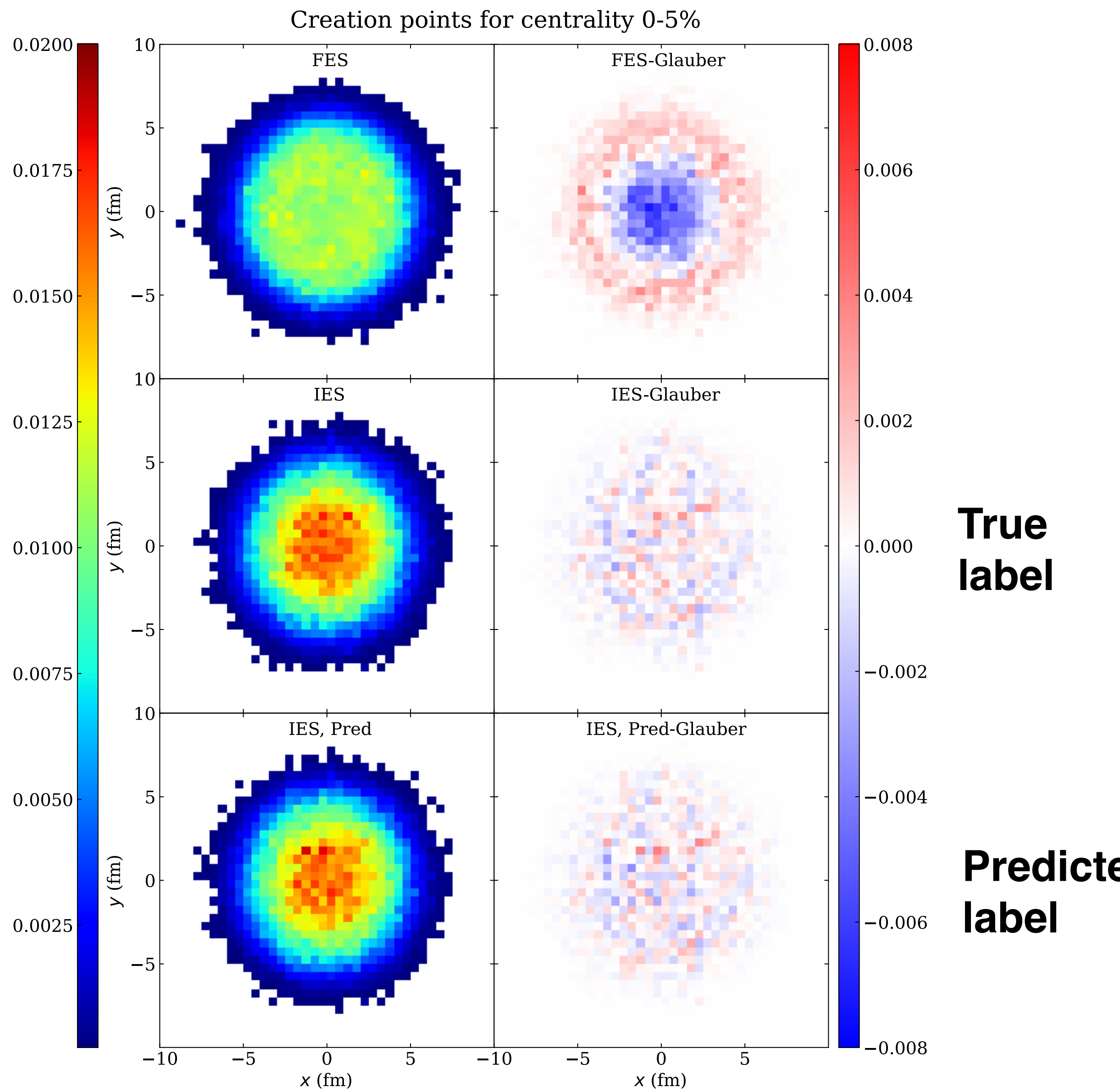


- Use jet images as inputs for CNN. Main result.
- Use jet observables as inputs for FCNN.
Mainly used for interpretability.

Good performance across
a wide range in χ

- Consistency check:
pp (vacuum) jets get $\chi \simeq 1$

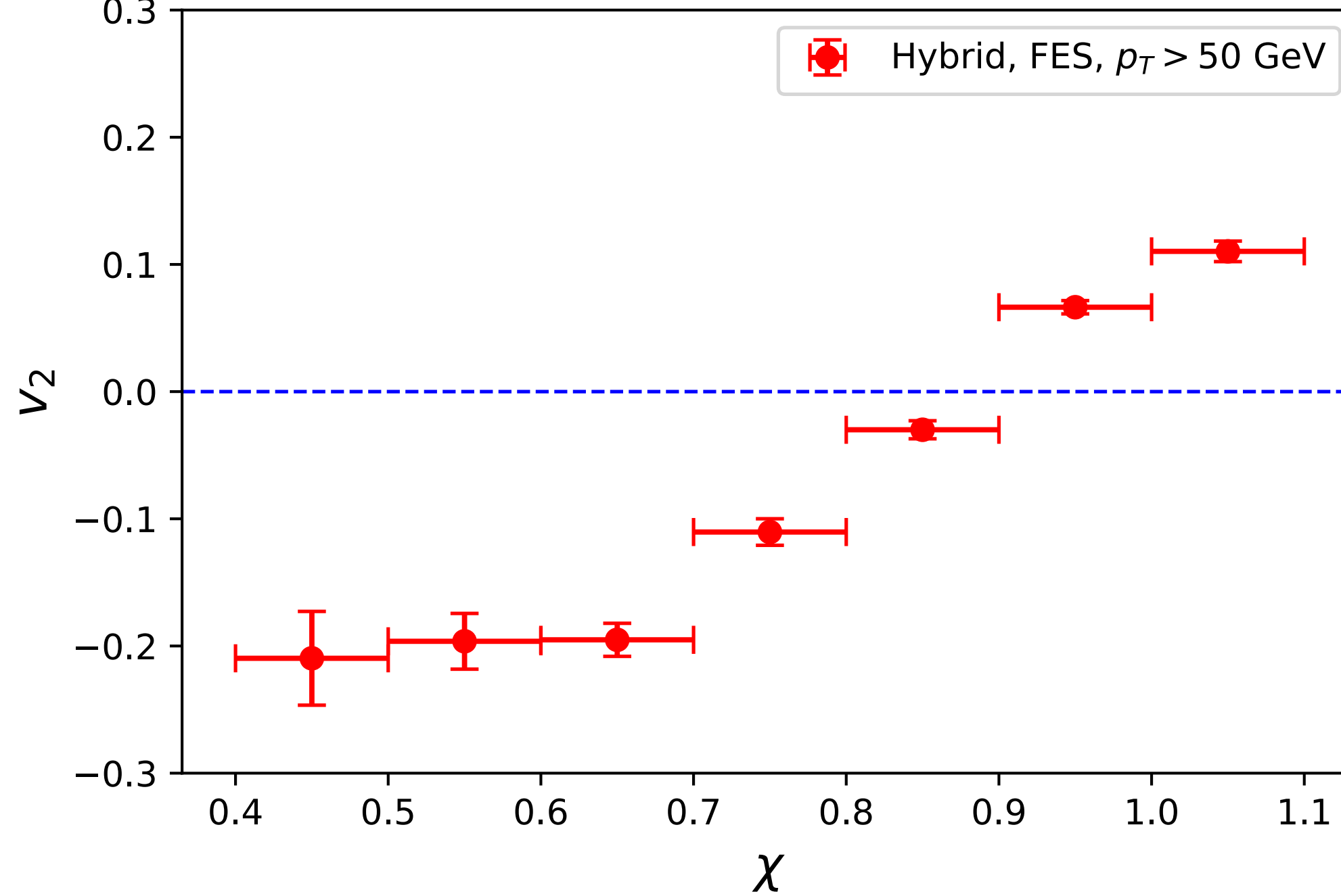
Accessing True Path Length Distributions



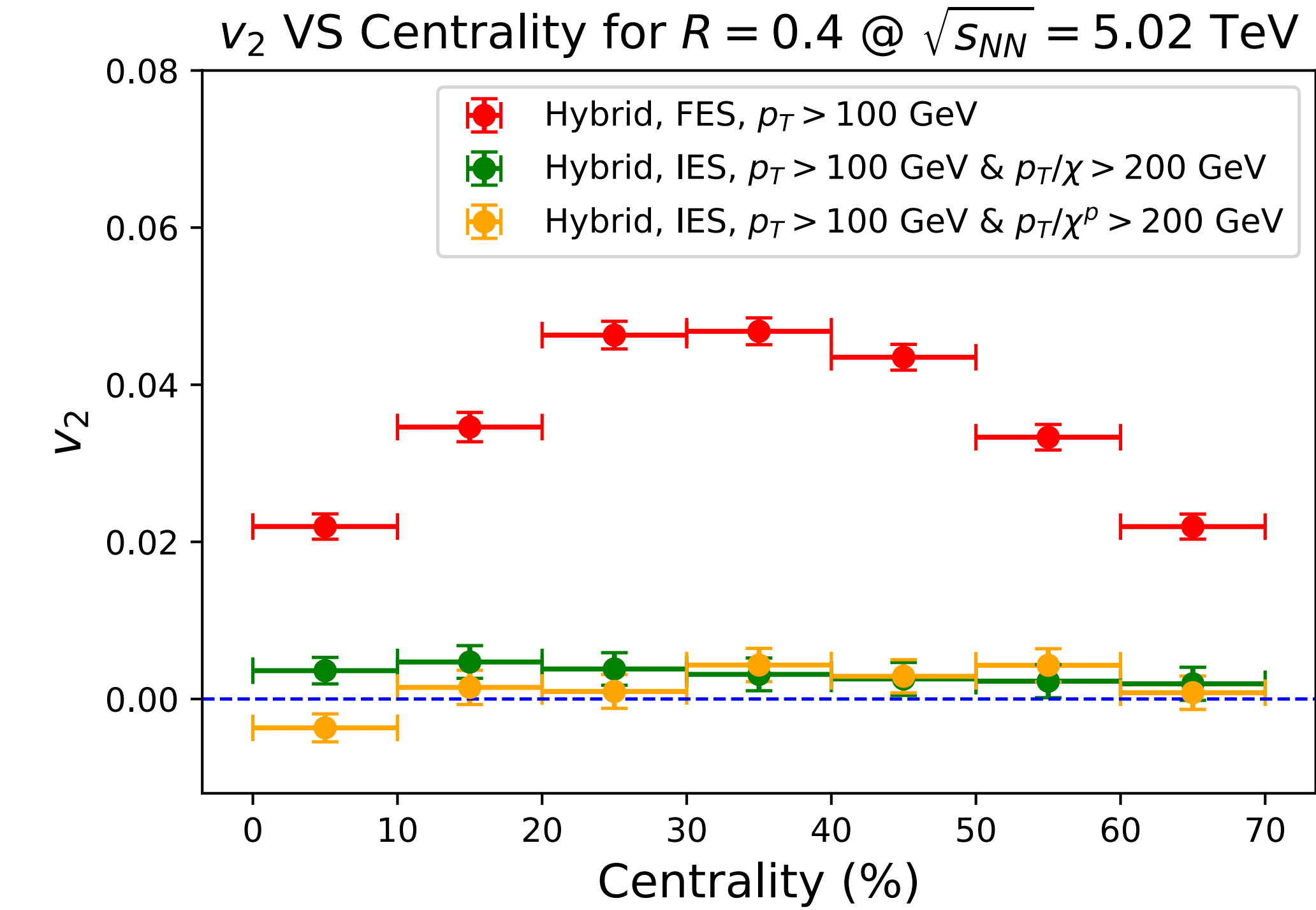
- **FES:** Select jets according to final energy.
 $E_f > E_{\text{cut}}$
 - Surface bias compared to actual nuclear overlap density.
- **IES:** Select jets according to “initial” energy.
 $E_f/\chi > E_{\text{cut}}$
 - Production point density unbiased w.r.t. true underlying distribution.

Accessing Initial Jet Anisotropies

v_2 VS χ for centrality 30-40%,
 $R = 0.2$ @ $\sqrt{s_{NN}} = 2.76$ TeV



Du, DP, Tywoniuk - PRL '21



- Intuitive origin of high- p_T jet anisotropies:

Small χ (large energy loss):
 → longer path length;
 → $v_2 < 0$.

and viceversa for large χ .

- However, if use IES:
 Reveals initial azimuthal anisotropies.
 In this model: none → $v_2 \sim 0$.

And in experiments?

Tomography with Deep Learning

Determination of production point in transverse plane.

Differential in:

- Orientation w.r.t. event plane.
- Energy loss ratio χ .

Production points **swap** in order to traverse more medium with increasing energy loss.

